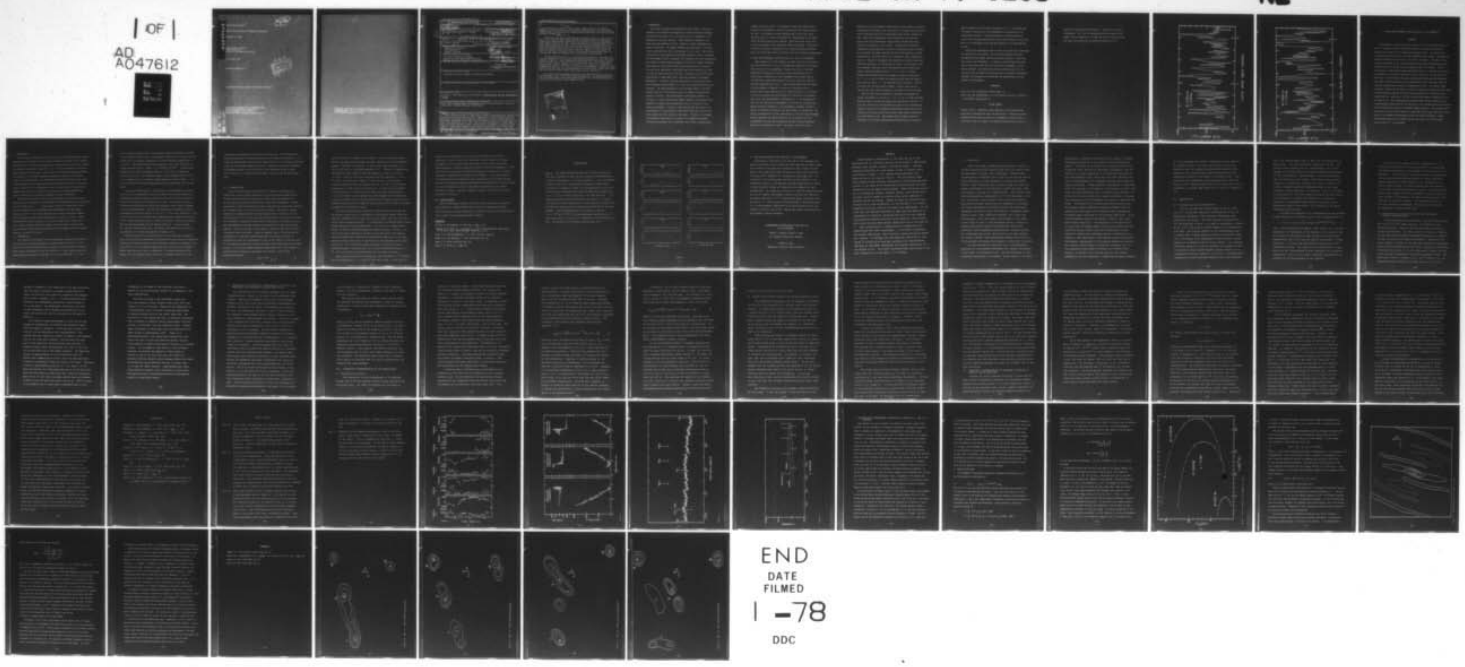
AD-A047 612 TUFTS UNIV MEDFORD MASS DEPT OF PHYSICS F/G 3/2
FINE SCALE RADIO STUDIES OF THE SUN.(U)
OCT 77 K R LANG F19628-76-C-0280
UNCLASSIFIED SCIENTIFIC-1. AFGL-TR-77-0208 NL

| OF |
AD
A047612



END
DATE
FILMED
1 -78
DDC

AD A047612

AFGL-TR-77-0208

FINE SCALE RADIO STUDIES OF THE SUN

Kenneth R. Lang

Department of Physics
Tufts University
Medford, Massachusetts 02155

15 October 1977

DDC
RECEIVED
DEC 14 1977
F

Scientific Report No. 1

Approved forpublic release; distribution unlimited

AIR FORCE GEOPHYSICS LABORATORY
AIR FORCE SYSTEMS COMMAND
UNITED STATES AIR FORCE
HANSCOM AFB, MASSACHUSETTS 01731

AD NO.
DDC FILE COPY

Qualified requestors may obtain additional copies from the Defense Documentation Center. All others should apply to the National Technical Information Service.

SECURITY CLASSIFICATION OF THIS PAGE (When Data Entered)

REPORT DOCUMENTATION PAGE

READ INSTRUCTIONS BEFORE COMPLETING FORM

1. REPORT NUMBER: AFGL-TR-77-0208	2. GOVT ACCESSION NO.
3. RECIPIENT'S CATALOG NUMBER	
4. TITLE (and Subtitle): FINE SCALE RADIO STUDIES OF THE SUN,	5. TYPE OF REPORT & PERIOD COVERED: Scientific ~~Report No. -1~~ 1 Aug. 1976 - 1 Oct. 1977
	6. PERFORMING ORG. REPORT NUMBER
7. AUTHOR(s): Kenneth R. Lang (Rept. for 1 Aug 76 - 1 Oct 77)	8. CONTRACT OR GRANT NUMBER(s): F 19628-76-C-0280
9. PERFORMING ORGANIZATION NAME AND ADDRESS: Department of Physics, Tufts University, Medford, MA 02155	10. PROGRAM ELEMENT, PROJECT, TASK AREA & WORK UNIT NUMBERS: 4643-03-02, 62101F
11. CONTROLLING OFFICE NAME AND ADDRESS: Air Force Geophysics Laboratory, Hanscom Air Force Base, Bedford, MA 01731, Contract Monitor: Ronald M. Straka/PHP	12. REPORT DATE: 15 Oct 1977 13. NUMBER OF PAGES: 59 (68 p.)
14. MONITORING AGENCY NAME & ADDRESS (if different from Controlling Office)	15. SECURITY CLASS. (of this report): Unclassified 15a. DECLASSIFICATION/ DOWNGRADING SCHEDULE

16. DISTRIBUTION STATEMENT (of this Report)

Approved for public release, distribution unlimited

17. DISTRIBUTION STATEMENT (of the abstract entered in Block 20, if different from Report)

18. SUPPLEMENTARY NOTES

Portions of this report will be published in Solar Physics and the Astrophysical Journal

19. KEY WORDS (Continue on reverse side if necessary and identify by block number)

Solar Radio Interferometry, Fine Angular Scales, Flare Prediction, Quiet Sun, Active Sun, Sunspots, Granules, Solar Radio

20. ABSTRACT (Continue on reverse side if necessary and identify by block number)

Major flare eruptions in solar active regions create geophysical disturbances which may seriously disrupt Air Force communication and surveillance systems. This report discusses interferometric observations of solar active regions at centimeter wavelengths which show that the emission comes from sources which are only a few seconds of arc in size. The circular polarization of these small-scale features indicates a direct connection with the magnetic fields in active regions. Significant changes in the circular polarization of the fine scale regions only occurs in the few hours prior to flare eruptions. (cf. Lang, K.R.,

next page

DD FORM 1 JAN 73 1473 EDITION OF 1 NOV 65 IS OBSOLETE

403317

SECURITY CLASSIFICATION OF THIS PAGE (When Data Entered)

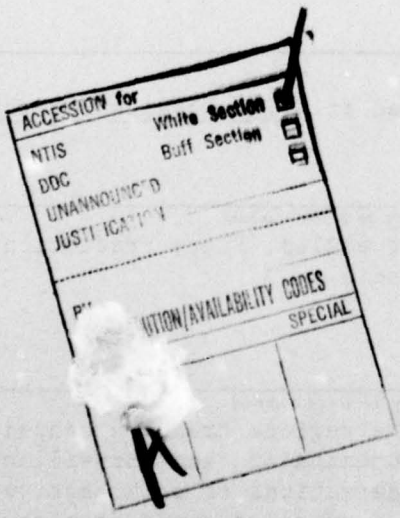
20.

Solar Physics 52, 63 (1977)). This result suggests that it is changes in magnetic field configurations which trigger flare emission, and that routine observations of the small-scale trigger sources might lead to a reliable flare forecast technique.

During the past year the Sun has been relatively inactive, and as long as the Sun is quiet the small-scale features have been found to be remarkably stable with angular sizes, intensities, and degrees of circular polarization which remain constant for days. This stability allows synthesis maps in which data taken during one day can be used to delineate the configurations of the small-scale structures within active regions. These structures can be used to study the magnetic field structures within the regions. In this report we describe the basic techniques used in constructing these synthesis maps and discuss maps taken on different days with different polarizations.

An additional byproduct of the observations discussed in this report has been the delineation of ubiquitous small-scale features which cover the entire surface of the Sun. These features are detectable only when the more intense active regions are not present on the visible solar disk. Our observations indicate that thermal radiators with angular sizes comparable to granules and supergranules exist in all parts of the visible chromosphere. Studies of these features may well lead to an understanding of the mysterious process which feeds the hot solar wind which always flows from the Sun to the Earth.

This report also discusses preliminary solar observations with the 8-mm interferometer run by the Jet Propulsion Laboratories. The large bandwidth of this instrument makes it the best available facility in the United States for studying the small-scale flare trigger sources.



A. INTRODUCTION

This report discusses interferometeric observations of the Sun at centimeter and millimeter wavelengths with angular resolutions between one and thirty seconds of arc (one second of arc is equivalent to 700 kilometers on the solar surface). When sunspots are present on the solar disk, they dominate the solar emission at these wavelengths and angular resolutions. The sunspot emission has been shown to come from a few sources which are only a few seconds of arc in size. The circular polarization of these small-scale features indicates a direct connection with the magnetic fields in sunspots, and changes in circular polarization are thought to reflect emerging magnetic fields which trigger subsequent flare emission. When these intense active regions are not present on the solar disk, ubiquitous, unpolarized small-scale features are found to cover the entire surface of the Sun. In Sections B and C we discuss observations of these small-scale, quiet-Sun features at centimeter wavelengths. In Section D similar observations of the quiet Sun with the 8 millimeter interferometer run by the Jet Propulsion Laboratory are discussed. The large bandwidth of this instrument makes it the best available facility in the United States for studying the small-scale features of the Sun. The interferometric observations reported in Sections B, C, and D indicate that thermal radiators with angular sizes comparable to granules and supergranules exist in all parts of the visible chromosphere. Studies of these features may well lead to an understanding of the mysterious process which feeds the hot solar wind which always flows from the Sun to the Earth. In Section E we discuss interferometric observations of sunspots at centimeter wavelengths. As long as the sunspots are not emitting solar flares, the small-scale

trigger sources are found to be remarkably stable with angular sizes, intensities, and degrees of circular polarization which remain constant for days. This stability allows synthesis maps in which data taken during one day can be used to delineate the configurations of the small-scale structures within active regions. These structures can be used to study the magnetic field structures within the regions. In Section E we describe the basic techniques used in constructing these synthesis maps, and discuss maps taken on different days with different polarizations.

B. SMALL SCALE FEATURES OF THE QUIET SUN AT 3.7 AND 11 cm WAVELENGTH

When sunspots (or active regions) are absent from the solar surface, the solar emission at 3.7 and 11 cm wavelength originates in the higher, hotter levels of the chromosphere. Because this layer of the solar atmosphere lies between the optically visible photosphere and the solar corona, observations of the chromosphere may provide clues to the mysterious process which heats up the solar corona and feeds the outwardly expanding solar wind. It has long been known that the underlying photosphere is composed of a matrix of convection cells or granules which have preferred sized of 2,000 km (700 km = 1 arc second on the solar surface) and which pulsate with periods of a few minutes. Lang (1974) used interferometric observations at 3.7 cm wavelength to show that the entire solar chromosphere is covered with features whose angular sizes are comparable to the photospheric granules, and which appear to fluctuate in intensity with time scales of a few minutes. The natural interpretation of these observations is that the radio-wavelength features represent the upward projection of the granules into the chromosphere, and that the fluctuations represent outward travelling waves which feed the solar corona. Of course, variations in the

amplitude of an interferometer fringe pattern can be caused by intrinsic fluctuations of the small-scale structures or by complex source structure whose orientation within the interferometer beam pattern changes with time. Kundu and Alissandrakis (1975) observed the quiet Sun near equinox when the interferometer fringe pattern becomes effectively fixed and unchanging at source transit. Because fluctuations were observed at transit, they have to be due to variations within the small-scale features, but Kundu asserted that the variations have no unique periodicities. We believe that this is because he added together data taken at a variety of wavelengths and resolutions to obtain noise like amplitude variations. As illustrated in Figure 1 and discussed in the next paragraph, intrinsic source fluctuations are only visible with angular resolutions smaller than 3.5 " (λ = 3.7 cm, B = 2100m). Because the fluctuations are more intense at angular resolutions of 2.7 " (λ = 3.7 cm, B = 2700m) the variable sources must have angular sizes which are about 3 " - the preferred size of granules. Moreover, we believe that the data shown in Figure 1 exhibit quasi-periodic fluctuations, and a Fourier analysis of this data is now in progress.

When the quiet Sun is observed at centimeter wavelengths with angular resolutions of 10.5 and 36.7 " (λ = 11 cm, B = 2100m and 600m), different types of ubiguitous, small-scale features are observed. In this case variations in the amplitude and phase of the interferometer signal are caused by the changing interferometer fringe spacing while viewing a few intense, small-scale features whose angular separations are a few minutes of arc. The angular sizes of these sources are comparable to the larger supergranulation network seen in the photo-

sphere (preferred cell size about 35,000 km or 50 "). We believe that the larger features seen in the chromosphere are extensions of the supergranular pattern. A detailed discussion of these features is given in the following paper entitled "Small Scale Features of the Quiet Sun at 11 cm Wavelength" which has been submitted to the Astrophysical Journal.

Because the supergranules seen at both optical and radio wavelengths are stable and do not pulsate, they are ideal candidates for radio synthesis maps which might show the well-ordered matrix of convection cells seen in the photosphere. In addition, time averaged data might lead to radio maps which show the lattice-like arrangement of photospheric granules. Such maps would provide conclusive proof for our conjecture that the small-scale features seen at centimeter wavelengths represent the extensions of the granules and supergranules into and through the chromosphere.

REFERENCES

Lang, K.R. 1974, Astrophysical Journal 192, 777.

Kundu, M.R. and Alissandrakis, C.E. 1975, Monthly Notices of the Royal Astronomical Society 173, 65.

FIGURE LEGENDS

Figures 1 and 2: Variations in the amplitude of the interferometer signal while observing the quiet Sun near equinox. Because the interferometer fringe spacing is fixed and unchanging at source transit (Zero hours local hour angle), the observed variations must be due to

intrinsic fluctuations of small-scale 3 " features in the solar chromosphere. Note that the variations are more intense at the longer effective baseline, B = 2700m, and that the variations are well above the theoretical rms noise fluctuation of 10 Jy.

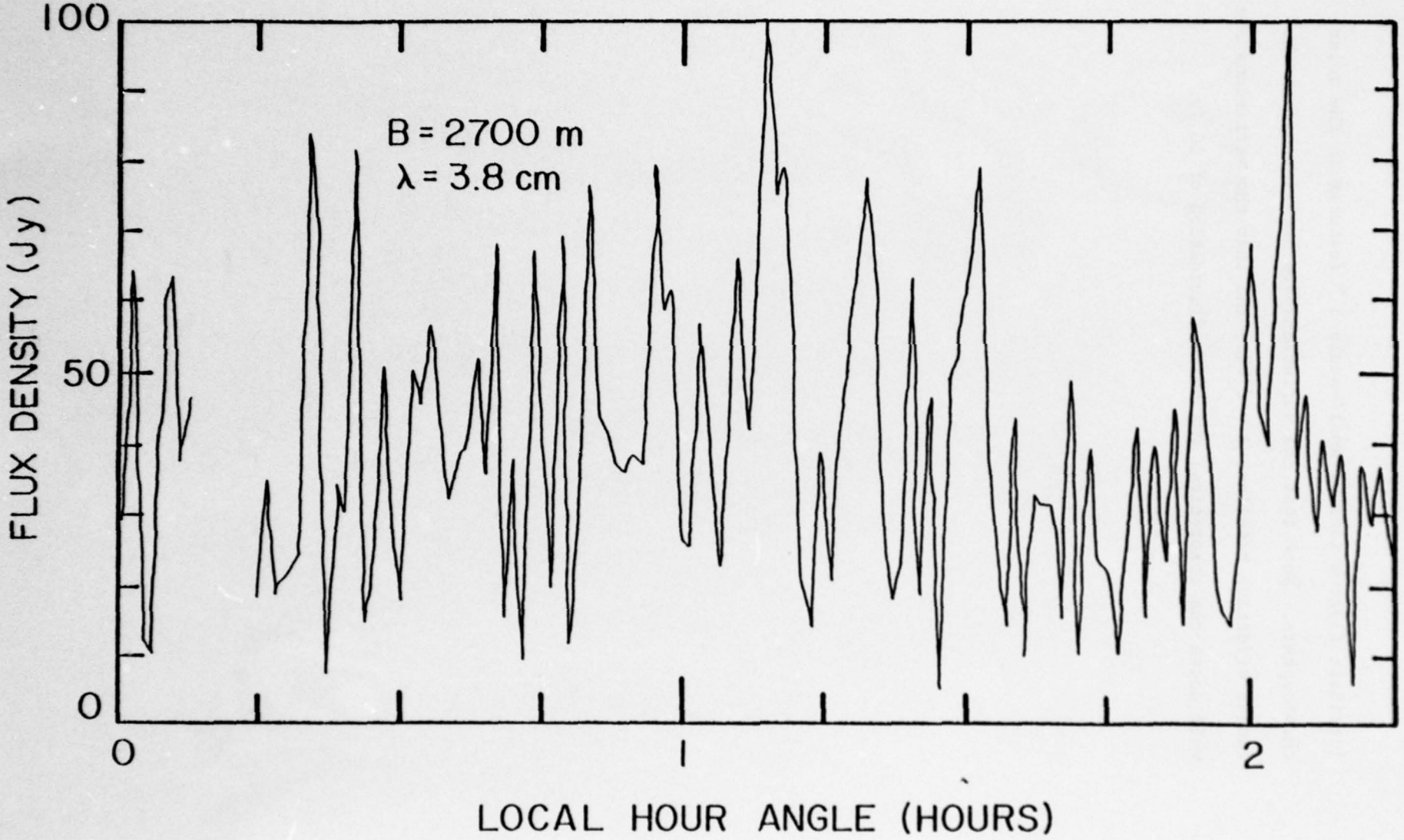

100
50
0
FLUX DENSITY (Jy)
B = 2700 m
λ = 3.8 cm
0
1
2
LOCAL HOUR ANGLE (HOURS)

Figure 1.

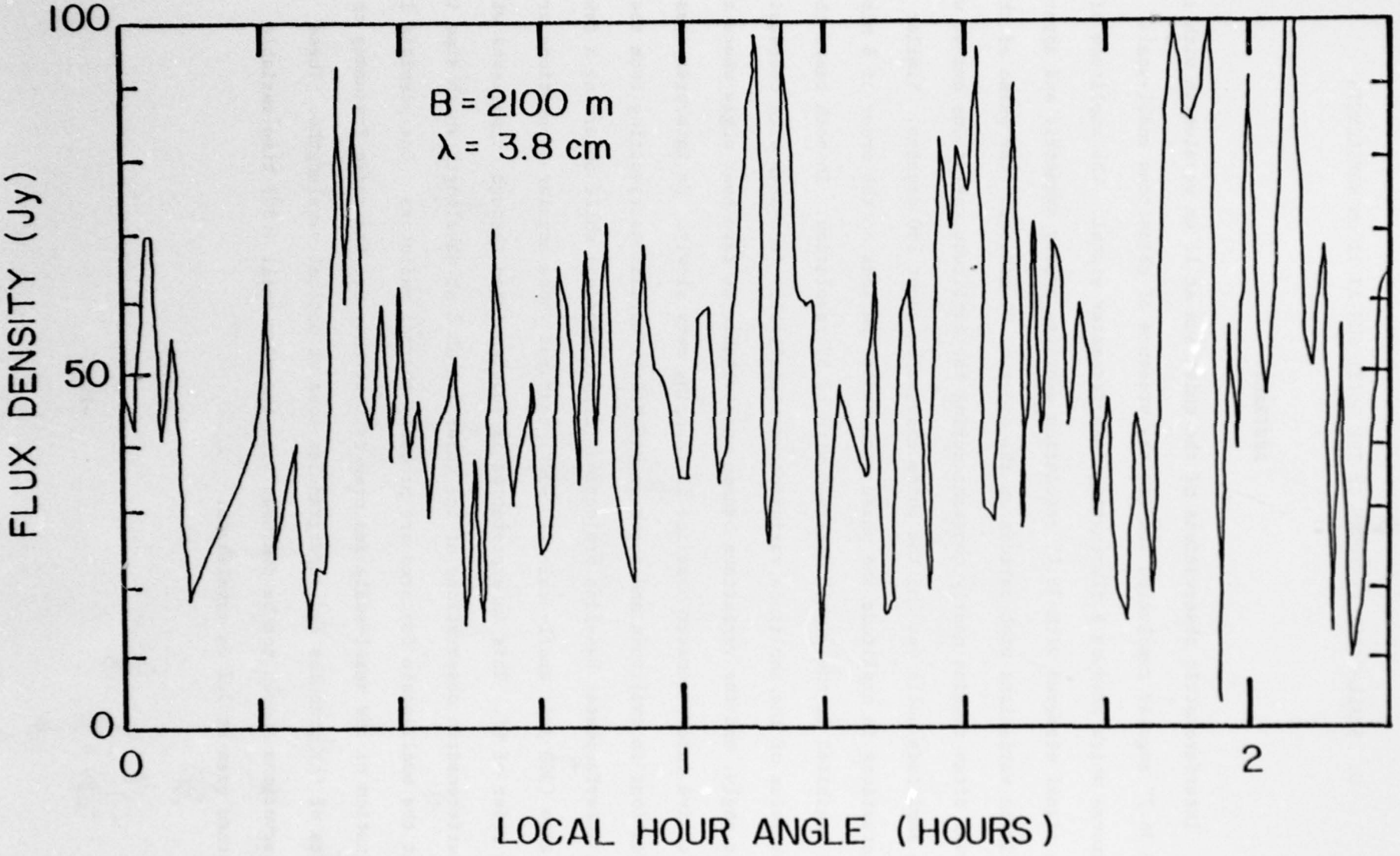

100
50
0
FLUX DENSITY (Jy)
B = 2100 m
λ = 3.8 cm
0
1
2
LOCAL HOUR ANGLE (HOURS)

Figure 2.

C. SMALL-SCALE FEATURES OF THE QUIET SUN AT 11 cm WAVELENGTH

ABSTRACT

Interferometric observations of the quiet Sun at 11 cm wavelength with 10.5" and 36.7" angular resolution confirm the presence of ubiquitous small-scale features which produce a fluctuating interferometer signal. The amplitude of the signal observed with 36.7" resolution exhibits nearly symmetric and apparently periodic variations with periods on the order of 20 minutes. The phase of the signal often remains nearly constant during the amplitude variations except when the amplitude nulls out and the phase changes by about 180 degrees. Similar fluctuations in amplitude and phase with faster periods on the order of 6 minutes are exhibited in the signal observed with 10.5" resolution. In both cases the peak value of the amplitude variations systematically decreases with decreasing hour angle, and the variations become undetectable at zero hour angle where the effective interferometer baseline is changing very slowly. We interpret these variations in amplitude and phase as visibility variations resulting from the changing interferometer baseline projection (fringe spacing) while observing a few intense (300 Jy), small-scale (10"-30") features whose angular separations are on the order of 6'. This interpretation is substantiated through comparisons with interferometric observations of the quiet Sun at 8 mm wavelength which also indicate that the small-scale features are probably thermal radiators. One possible interpretation of the small-scale features is that they are the radio frequency counterparts of the granules and supergranules seen at optical wavelengths. These observations should not be confused with the very small (< 3") time variable sources seen at 3.7 cm wavelength.

I. INTRODUCTION

Interferometric observations of the quiet Sun at 8 mm wavelength with angular resolutions on the order of 30 arc seconds (Bocchia and Poumeyrol, 1976; Jannsen, Olsen and Lang, 1977) show the ubiquitous small-scale features previously observed at centimeter wavelengths by Lang (1974 a, b). The solar emission at 8 mm wavelength originates in the deeper, cooler layers of the solar chromosphere whereas the radiation of the longer centimeter wavelengths originates in the higher, hotter chromospheric layers. The observations of similar features at both wavelengths suggests that the small-scale features extend from the top of the photosphere through most of the chromosphere, and the similarities in angular sizes suggests that they may be related to the granules and supergranules seen at optical wavelengths in the upper photosphere and lower chromosphere.

The amplitude and phase of the 8 mm interferometric signal undergo unique variations with time scales of 10-30 minutes often punctuated with nulls associated with 180° phase shifts. In this paper we report the observation of very similar variations at 11 cm wavelength with approximately the same angular resolution (36.7"). The reduced intensity at the longer wavelengths suggests that the radiation from the small-scale regions is thermal in origin. These observations and those obtained at 11 cm with a higher angular resolution of 10.5" provide further evidence for Jannsen, Olsen and Lang's conclusion that the variations in amplitude and phase are due to the changing effective baseline caused by the Earth's rotation.

II. OBSERVATIONS

The observations were made with the three-element interferometer system at the National Radio Astronomy Observatory between March 30 and April 4, 1977. Three 25.9-m diameter paraboloids were placed on a skewed baseline with linear phase center displacements of 600, 2100 and 2700 m. A dual channel system was used at signal frequencies of 2695 MHz (λ = 11 cm) and 8085 MHz (λ = 3.7 cm)

with circularly polarized feeds, an intermediate frequency bandwidth of 30 MHz, and an integration time of 30 s. The parametric amplifiers were bypassed and the system noise was completely dominated by the solar brightness temperatures of 2×10^4 K. Under these conditions the theoretical r.m.s. noise fluctuation in fringe amplitude was 10 Jy, where 1 Jy = 10^{-23} erg $s^{-1} cm^{-2} Hz^{-1}$. The half power beamwidth of the main interferometer beam at λ = 11cm was 14', whereas the angular resolutions of the individual fringes at this wavelength were 36.7" and 10.5", respectively, for the 600m and 2100m baselines at source transit. It is the data obtained with these configurations which are the primary topic of this paper.

The antennae were pointed at the Sun center at the beginning of each day, and the point of intersection of the line of sight with the solar surface was subsequently tracked by computer correction for the drift of the Sun across the sky and for the rotation of the Sun about its axis. In all cases the entire visible solar surface was quiet without any optically visible signs of sunspots or other disturbed regions. The data were calibrated by observing 3C 84 which was assumed to have a flux density of 19 Jy at λ = 11cm, and by measuring a value of ten for the ratio of the system noise temperatures while observing the Sun and 3C 84. Typical calibrated data are illustrated in Figure 1 where we also include 8mm quiet Sun data obtained with 30" angular resolution a few days earlier (cf. Jannsen, Olsen and Lang, 1977) and sunspot data obtained with the N.R.A.O. interferometer in the same configuration in November, 1975.

Interpretations of this data are given in the next selection, and here we point out that the major variations in the amplitude and phase cannot be instrumental. The amplitude variations cannot be noise fluctuations because the theoretical r.m.s. noise level is 10 Jy, and because similar variations are absent when tracking a sunspot where the noise levels are comparable. The sunspot observations also suggest that the variations cannot be caused by a changing orientation of the

interferometer sidelobes which view the entire solar disk. This conclusion was further substantiated by observing the Moon with the parametric amplifiers in. No signal was detected from the Moon with an upper limit of 0.5 Jy although the Moon has roughly the same angular diameter as the Sun. Taking into account the difference in brightness between the Sun and the Moon, this observation places an upper limit of about 20 Jy to variations which might be produced from the entire solar disk.

III. INTERPRETATIONS

The quiet Sun data taken with 30" and 36.7" resolution at 8mm and 11cm, respectively, exhibit similar variations in amplitude and phase suggesting that the small-scale features which give rise to these variations commonly occur on the quiet Sun and extend throughout most of the solar chromosphere. Because interference fringes were detected, the signals must come from small-scale structures $\lesssim$30" in angular size (1" = 700 km on the solar surface). The optically visible granules and supergranules have respective angular sizes of seconds of arc and tens of seconds of arc, and they are also always present on the surface of the Sun. It is tempting to interpret the small-scale features seen at millimeter and centimeter wavelengths as the radio frequency counterparts of the granules and supergranules. If this is the case, we would expect a lattice of small-scale features covering the entire solar disk. Under the assumption that a few intense sources predominate in a given main interferometer beam, the observed variations in amplitude and phase can be interpreted in terms of the visibility variations caused by the changing interferometer baseline projection while observing the more intense sources. If the typical angular spacing of these sources is θ, then we expect to observe periodic variations in amplitude with a period, P, given by the approximate expression

$$P \approx 4 \times 10^4 \quad \frac{1}{\theta} \quad \frac{\lambda}{B} \quad , \qquad (1)$$

where the period is in seconds, θ is in radians, λ is the observing wavelength, and B is the linear distance between the phase centers of the two interferometer elements. Choosing P = 30 minutes, λ = 11cm, and B = 600m, we obtain $\theta \simeq 6'$. This is well within the half-power beamwidth of 14'. Equation (1) suggests that variations with similar periods should be observed at λ = 8mm, B = 60m and λ = 11cm, B = 600m, and that faster variations should be observed at λ = 11cm, B = 2100m. As illustrated in Figure 1, this is the case. The five minute variations observed by Kundu and Velusamy (1975) at λ = 1.3cm, B = 265m further substantiate the trend inferred from equation (1). The fact that the intensity of the variations at λ = 8mm are about 20 times larger than those observed at λ = 11cm with roughly the same angular resolutions suggests that the small-scale sources are thermal radiators, although observations at identical times with interferometers with identical main beams and fringe spacings would be needed to determine the spectrum of the radiation exactly.

The quiet Sun observations illustrated in Figure 3 were all taken when the Sun was near equinox where the interferometric fringe pattern becomes effectively fixed and unchanging within the main beam at source transit (zero local hour angle and zero degrees source declination). It is here that the variations shown in Figure 1 become undetectable, adding further support to the view that a changing fringe pattern (or effective baseline) produces the observed variations. Moreover, this view is additionally supported by the fact that the peak value of the amplitude variations systematically increase with increasing hour angle, and that the phase remains relatively stable except at amplitude nulls where 180 degree phase changes often occur. All of these facts support our general conclusion that we are observing visibility variations from a set of ubiquitous small-scale sources of 10" - 30" in size which are distributed all over the surface of the Sun.

These variations should not be confused with time variations of 2 - 20 minutes which are observed with λ = 3.7 cm and B = 2100 and B = 2700m. In this case, the

sources are a few seconds of arc in size and any complex source structure would have to be well outside the 5' main beam to cause variations of minutes. Furthermore, we have detected these variations at source transit during this observing session — providing additional evidence to Kundu and Alissandrakis' (1975) proof that they are not due to visibility variations, but rather due to intrinsic variations of emission from the second of arc features. It is these second of arc features which are comparable in size to granules and which probably undergo intrinsic time variations, whereas the features with angular sizes of tens of seconds of arc are comparable in size to supergranules and probably do not undergo intrinsic variations. Both sets of features, however, are distributed all over the surface of the Sun.

IV. ACKNOWLEDGMENTS

Radio interferometric studies of the Sun at Tufts University are supported under Contract No. F19628-76-C-0280 with the Air Force Geophysics Laboratory. The National Radio Astronomy Observatory is operated by Associated Universities,Inc. under contract with the National Science Foundation.

REFERENCES

Bocchia, R. and Poumeyrol, F. 1976, Ap. J. 204, L 107.

Janssen, M.A., Olsen, E. T. and Lang, K. R. 1977, "Interferometric Observations of the Quiet Sun at 8mm Wavelength" submitted to Ap. J.

Kundu, M. R. and Alissandrakis, C. E. 1975, M.N.R.A.S. 173, 65.

Kundu, M. R. and Velusamy, T. 1974, Solar Phys. 34, 125.

Lang, K. R. 1974a, Solar Phys. 36, 351.

Lang, K. R. 1974b, Ap. J. 192, 777.

FIGURE LEGENDS

Fig. 3. The signal amplitude and phase as a function of local hour angle while observing the quiet Sun near equinox with interferometers at a variety of wavelengths, λ, and linear baselines, B. Note the apparently periodic fluctuations in amplitude whose intensities systematically increase with increasing hour angle, and the phases which are relatively constant except at amplitude nulls where 180 degree phase changes often occur. Also note the faster variations at the longer baselines. For comparison purposes we show interferometric observations of a sunspot with relatively constant amplitude and a steady phase drift caused by the fact that the radio source is not centered in the main beam of the interferometer. Here the amplitude data are calibrated in Janskies ($1\ Jy = 10^{-23}\ erg\ s^{-1} cm^{-2} Hz^{-1}$) and the measurement uncertainties due to system noise alone is 30 Jy and 10 Jy, respectively, for the 8mm and 11cm data. The 8mm data are from Jannsen, Olsen and Lang (1977).

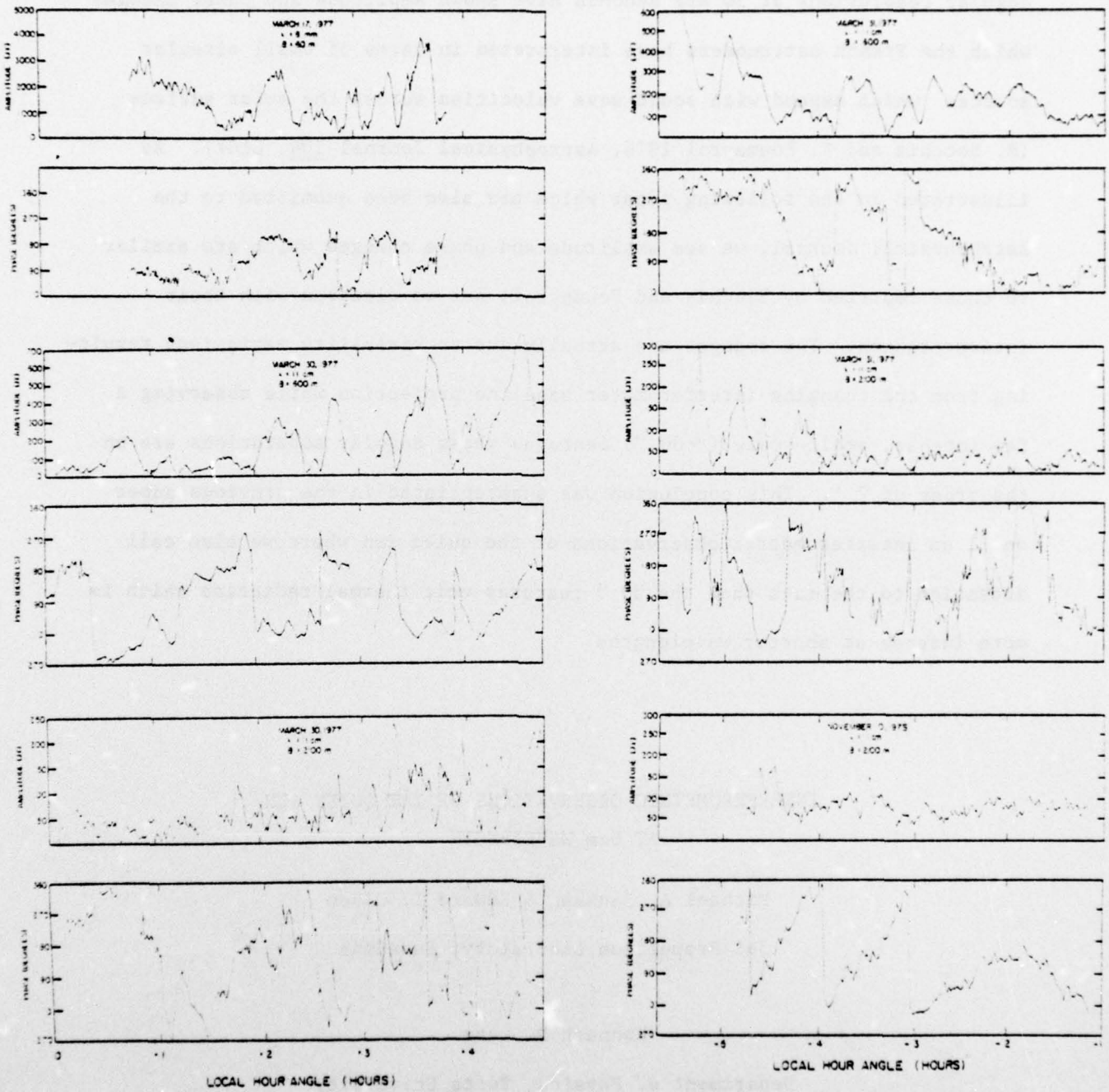


Figure 3

D. SMALL-SCALE FEATURES OF THE QUIET SUN AT 8 mm WAVELENGTH

Interferometric observations of the quiet Sun at 8 mm wavelength with angular resolutions of 30 arc seconds have shown amplitude and phase changes which the French astronomers have interpreted in terms of small circular sources which expand with sound wave velocities across the solar surface (R. Bocchia and F. Poumeyrol 1976, Astrophysical Journal 204, L107). As illustrated in the following paper which has also been submitted to the Astrophysical Journal, we see amplitude and phase changes which are similar to those reported by Bocchia and Poumeyrol; but we disagree with their interpretation. The changes are actually due to visibility variations resulting from the changing interferometer baseline projection while observing a few intense, small-scale ($\sim$30 ") features whose angular separations are on the order of 7 '. This conclusion was substantiated in the previous paper on 11 cm interferometric observations of the quiet Sun where we also call attention to the fact that the 30 " features emit thermal radiation which is more intense at shorter wavelengths.

INTERFEROMETRIC OBSERVATIONS OF THE QUIET SUN AT 8mm WAVELENGTH

Michael A. Janssen & Edward T. Olsen

Jet Propulsion Laboratory, Pasadena

Kenneth R. Lang

Department of Physics, Tufts University

ABSTRACT

Interferometric observations of the quiet Sun at 8.3 mm wavelength and 30" resolution confirm the existence of small-scale features which produce a strong, fluctuating signal. The most plausible explanation for this signal is that it results from a distribution of small (< 30") sources whose individual flux densities are on the order of 5000 Jy. The fluctuating signal often exhibits nearly periodic variations in fringe amplitude with periods in the range 10-30 minutes and with nulls which are often associated with 180 degree phase changes. These variations are not due to instrumental effects, although shorter, less intense fluctuations could be caused by tracking errors while observing an extended pattern of sources. Models in which the variations are entirely due to time variability in a few sources or to a single expanding source are ruled out or found to be implausible. We conclude that the observed variations in amplitude and phase may be interpreted as visibility variations resulting from the changing interferometer baseline projection while observing a few intense, small-scale features whose angular separations are on the order of 7'. This interpretation is substantiated by comparisons with observations with other interferometers at different wavelengths and angular resolutions. The visibility induced variations should not, however, be confused with the amplitude variations on time scales of minutes which have been recorded with interferometers operating at centimeter wavelengths with angular resolutions of a few seconds of arc. The latter variations might well be due to the time variability of a few small ($\leq$ 3") sources.

I. INTRODUCTION

Some of the more interesting solar features visible at optical wavelengths have angular sizes which are smaller than the beamwidths of single radio telescopes. Because radio interferometric techniques can be used to give angular resolutions comparable to those obtained at optical wavelengths, however, these techniques can be used to study the radio frequency counterparts of the optically visible granules, solar oscillations, spicules, and supergranules. Lang (1974a) first used interferometric observations at 3.7 cm wavelength to show that the entire visible surface of the quiet Sun contains small-scale features whose sizes are comparable to granules, and whose fluctuations in intensity often have time scales comparable to those of solar oscillations. Subsequent observations (Lang, 1974b; Kundu and Velusamy, 1974; Kundu and Alissandrakis, 1975; and Bocchia and Poumeyrol, 1976) made in the range of 8 mm - 11 cm wavelength and at a variety of spatial resolutions confirm the presence of small-scale structures which apparently produce strong, variable signals. The interpretations of the time variations of these signals has varied, however, with explanations ranging from the short lived spicules to sources which expand at sound wave velocities.

We have observed the quiet Sun with an interferometer operating at 8 millimeters wavelength with angular resolutions on the order of 30 seconds of arc. The solar emission at this wavelength originates in the deeper, cooler layers of the solar

chromosphere, whereas the radiation at the longer, centimeter wavelengths originates in the higher, hotter chromospheric layers. In Section II we confirm the ubiquitous small-scale structures first observed at centimeter wavelengths, and call attention to unique variations in the amplitude and phase of the interferometer signal which have also been observed with other interferometers with comparable angular resolutions and signal wavelengths. Nearly periodic fluctuations in amplitude occur with periods in the range of 10-30 minutes and with nulls which are often associated with 180 degree phase changes. In Section III we call attention to various incorrect or implausible explanations for the observed variations in amplitude and phase. Considerations of tracking and pointing errors and the changing signal received by antenna sidelobes from the entire solar disk lead to the conclusion that instrumental artifacts cannot give rise to the observed variations. Pointing and tracking errors could produce, however, more rapid, less intense variations. Considerations of the association of nulls with 180 degree phase shifts and the absence of variations at source transit when the interferometer fringe pattern is effectively unchanging make an interpretation in terms of a few small-scale, time-variable sources implausible. Furthermore, measurements of the antenna temperature received by a single antenna during the observed variations rule out the expanding source model of Bocchia and Poumeyrol (1975). Finally, in Section IV we conclude that the only tenable explanation for the variations in amplitude and phase observed

at 8 mm wavelength with angular resolutions on the order of 30 seconds of arc is that they are visibility variations resulting from the changing interferometer baseline while observing a few intense small-scale structures which are separated by angles on the order of 7 minutes of arc. This conclusion has subsequently been substantiated by Lang and Willson (1977) through observations of the quiet Sun at 11 cm wavelength at angular resolutions of 36.7 and 10.5 seconds of arc.

II. OBSERVATIONS

a) The Table Mountain Interferometer

The Sun was observed between March 15 and 20, 1977, with the 8 millimeter wavelength interferometer at the Jet Propulsion Laboratory's Table Mountain Observatory near Wrightwood, California. The Table Mountain interferometer will be described in detail in a paper in preparation (Janssen et al, 1977), and we give a brief summary of its characteristics here. The primary elements of the interferometer are a 5.5-meter and a 3-meter antenna located on an east-west baseline of 60 meters (7120 wavelengths) which provides a fringe spacing of 28 seconds of arc at source transit. The combined half-power beamwidth of the two antennas is 8 minutes of arc. The receivers employ double-sideband crystal mixers with an intermediate-frequency bandwidth of 350 MHz. A switched-delay compensation network maintains coherence over this bandwidth

with a net random signal loss of less than one percent due to delay error. The local oscillator frequency is 36 GHz. The natural output frequency of the interferometer, due to the passage of a source through the narrowly-spaced fringe pattern of the interferometer, varies between 0 and ~1 Hz depending upon the position of the source. This natural fringe rate is brought to an artificial, constant 0.5 Hz by the addition of a small, computer-controlled frequency offset in the local oscillator signal supplied to one receiver. The 0.5 Hz output is digitized with a 100 msec sampling interval, and the resulting information is stacked and analyzed in a computer to determine the integrated signal amplitude and phase over a preselected period constrained to be a multiple of the basic two-second signal period.

In general the response of an interferometer to an extended source brightness distribution $T_B(\eta,\xi)$ may be approximated as

$$V(u,v) = \int\int G_1(\eta,\xi)G_2^*(\eta,\xi)T_B(\eta,\xi)e^{i2\pi u\eta}e^{i2\pi v\xi}d\eta d\xi \qquad (1)$$

(e.g., see Christianson and Högbom, 1969) where u and v are the projections in wavelengths of the baseline on the plane of the sky, along the directions of right ascension and declination respectively, and η and ξ are the angular coordinates in these directions. G_1 and G_2 are the complex voltage gains of the respective antennas. The output of the interferometer is thus seen to be the instantaneous Fourier transform, at the spatial frequencies u and v, of the source brightness distribution as modified by the beam patterns of the antennas.

The output of the Table Mountain interferometer for a distributed source such as the Sun consists of the amplitude and phase corresponding to the complex visibility function of Equation 1. We note that in the Table Mountain interferometer the relative phase difference between the local oscillator signals appearing at each receiver is not maintained by an active control system, but rather depends upon the stability of the local oscillator distribution system. The actual phase drift rarely exceeds 10°/hour as measured on point sources of known position; nevertheless, the absolute phase of the interferometer is typically unknown. The measured quantity is thus the visibility of Equation 1 multiplied by an unknown but effectively constant phase term.

b) Observations of the Quiet Sun with the 8 mm Table Mountain Interferometer

The observations were made during a six-day period around the time of the 1977 vernal equinox. We observed the Sun center exclusively, which at the time was quiet and clear of visible disturbances. All data are shown in Figure 1, comprising the amplitude and phase measurements obtained as a function of time on each of five days of observation. Except for the first interval on March 15, the data are plotted from contiguous thirty-second integrations of the signal, obtained in continuous intervals varying from 1-1/2 to 4 hours each in length (in the first interval we employed a ten second integration time). The amplitude is shown in Janskys (1 Jy = 10^{-26} w/m^{2}Hz); i.e., an unpolarized point source with a total output of 1 Jy would

produce a response of unit magnitude on the amplitude scale. The flux scale calibration is based on observations of Venus, for which we have taken an unresolved disk temperature of 465 K (Janssen, 1973). All amplitudes have been corrected for atmospheric attenuation, which amounts to 3% at the zenith. The measurement uncertainty for each 30 sec integration due to system noise alone was in all cases less than 30 Jy, and is negligible on the scale of Figure 4.

As a check on system performance, as well as for the purpose of calibration, we obtained the records on Venus which are shown in Figure 5. Venus was near inferior conjunction and was resolved by the interferometer. The records show the visibility function of Venus in the neighborhood of its first zero crossing. At this point the real part of the visibility function passes from positive to negative values, which is equivalent to a null in the visibility amplitude with a 180° phase inversion. The amplitude scatter of approximately 10 Jy is consistent with the system noise temperature of 1000 K, with the mean amplitude following the expected visibility function for Venus. The phase scatter is approximately given by $\Delta\theta = \sigma/a$, where σ is the amplitude scatter for large amplitude, and a is the amplitude. While the mean phase is consistent with a small or negligible phase drift, we note that the phase scatter does not decrease inversely with the amplitude beyond $a \approx 100$ Jy. This is known to be primarily due to small-scale inhomogeneities in the

atmosphere in the beams of the antennas, and gives a measure of the minimum phase scatter to be expected in the solar observations.

The data of Figure 4 are dominated at early and late hour angles by large "events" which occur over time scales of 10 to 30 minutes. These give the appearance of a quasiperiodic form, in several instances accentutated by sharply defined nulls in the signal amplitude. The duration of a large amplitude event is generally associated with a constant or smoothly varying phase where the phase scatter is consistent with the expected minimum. Several cases are present in which deep nulls are associated with phase shifts at approximately 180°. There is a marked association of the large, rapid events with time. They occur only at early and late hour angles, and are either absent or greatly diminished in the hour or so around transit. As discussed in more detail in the following sections, we believe the absence of these events at transit is due to the fact that they are caused by a changing effective baseline which becomes effectively fixed and unchanging while observing the Sun at transit when it is near the vernal equinox. Superimposed upon these large events are smaller scale variations in both phase and amplitude which nevertheless exceed the instrumental noise by a significant margin.

c) Comparisons with Quiet Sun Observations at 8 mm and 13 mm Wavelength with Comparable Angular Resolutions

Our observations can be directly compared with two other interferometeric studies of the quiet Sun at millimeter wavelengths. Bocchia and Poumeyrol (1974, 1976) have obtained extensive solar data using the 8 millimeter interferometer at Bordeaux (Delannoy et al, 1973), the frequency and baseline of which are effectively identical to that of Table Mountain. The Bordeaux interferometer employs smaller antennas and the main beamwidth is approximately 50% greater. Kundu and Velusamy (1974) observed the quiet Sun on several days with the fixed-baseline Hat Creek interferometer (Hills et al, 1973) at a wavelength of 13 millimeters. The Hat Creek interferometer employed dissimilar antennas yielding an effective beamwidth comparable to the Table Mountain interferometer. The antennas were located on a skewed baseline approximately three times longer in wavelength. The observations made with these two instruments did not include the special condition of invariant fringes which we obtained around transit. Our results away from transit bear striking similarity to their published data. Bocchia and Poumeyrol note many fluctuations with lobe-like structure, punctuated with nulls associated with 180° phase shifts. The 10-30 minute time scale of their events is comparable to the time scale of events we observed. Since they observed primarily the edge of the Sun their effective beam size containing source structure was more nearly comparable to ours. The Hat Creek data obtained by Kundu and Velusamy are observed to contain periodicities on the order of 5-8 minutes,

which differs by a factor well matched by their increased baseline and the corresponding increase in the rate of change of fringe spacing.

The typical amplitudes of events in both the Hat Creek and Bordeaux observations are presented in terms of antenna temperature, to which we may make comparison by employing the relationship

$$T_A = (A_1 A_2)^{1/2} \frac{S}{2k}$$

where A_1 and A_2 are the effective aperture areas of the two interferometer elements and S is the source flux. The amplitudes of our events are in the range $T_A \approx$ 15-25 K, and are well matched by the Bordeaux results $5K \leq T_A \leq 10$ K when we account for the difference in antenna sizes. The Hat Creek amplitudes are in the range 10-15 K for events observed with comparable baseline projections, falling to 5 K at their baseline transit. Their results are somewhat smaller, and the discrepancy may be due to the longer wavelength at which they observed. The similarity among these sets of observations lead us to conclude that all three interferometers are observing the same phenomena.

III. ALTERNATIVE INTERPRETATIONS OF THE OBSERVATIONS

a) Instrumental Artifacts

The observation by an interferometer of an extended source such as the Sun presents certain unique problems which we outline here. One class of artifacts can be caused by

tracking or pointing errors. Short-term tracking errors for the individual Table Mountain antennas, for example, may reach 0.5', whereas our failure to correct for solar rotation resulted in a long-term systematic drift of the observed sources at a rate of 1' per eight hours. In addition, systematic pointing errors accumulating over periods of minutes to hours may amount to 1'. A point source nominally positioned at the beam centers would suffer a signal loss up to 3% if both antennas were in maximum error in the same direction. The signal variation for a source near the beam half-power point, on the other hand, could reach ± 30% in this case. The typical rapid variations of the data in Figure 1 occurring over time scales of a few minutes are seen to have a peak-to-peak amplitudes less than 1500 Jy. A single source of 2500 Jy contribution near the half-power point of the beam could produce fluctuations of this magnitude. Furthermore, it is possible that longer term variations such as the slow variations around transit seen in Figure 1 are due to systematic long-term pointing variations. Although pointing and tracking errors may produce the weaker variations shown in Figure 1, they cannot produce the strong variations in which amplitude nulls are correlated with 180 degree phase changes.

A second class of artifacts may be generated by the brightness of the entire Sun as shaped by the beam pattern function $G_1 G_2^*$. We must consider the second-order effects generated by the integration outside the main beam since they are effectively multiplied by the total solar flux. The

pattern $G_1 G_2^*$ of the Table Mountain interferometer may be approximated by a Gaussian distribution which represents the main sun-centered beam superimposed on the beam sidelobes which view the uniformly bright disk of the Sun. Although the sidelobes at 10' to 16' from the beam center are measured to possess a more-or-less smooth gain within the range 17-20 db below the main beam, the symmetrical main beam views a constant flux from the unperturbed Sun and it is the changing orientation of the sidelobes which may produce a variable signal. The transform of the uniform disk component obtained from equation (1) is

$$V_{disk}(w) = \sqrt{\frac{8}{\pi}}\, \bar{G}\, S_o (2\pi wR)^{-3/2} \cos\left(2\pi wR - \frac{3\pi}{4}\right), \qquad (2)$$

where the total contributed flux from the disk, $\bar{G}\, S_o$, is the main sidelobe gain times the total solar flux, S_o, the apparent solar semidiameter is R, and w is the magnitude of the baseline projection. Hence, we have assumed that $wR \gg 1$ because wR varied through the range 12-33 during the course of the observations. Equation (2) predicts peaks in the measured visibility at intervals of $\Delta w \approx 100$ whereas the observed variations occur at intervals of $\Delta w \approx 500$. Assuming a Sun brightness temperature of 8700 K and a mean sidelobe gain $\bar{G} = 0.01$, the amplitudes of the peaks vary from 120 Jy near transit to as much as 600 Jy near the hour angle limits of the present observations. Although this component is neither of sufficient amplitude nor of the correct frequency to explain the observations, it may be expected to add significantly to the measured signal.

In addition, for an interferometer employing identical antennas of good quality one will expect sharp, ring-shaped nulls concentric with the main beam. The transform of a dark ring of radius R' which may be consequently impressed on the solar disk may be found from Equation 1 to be of the form

$$V_{ring}(w) \approx \sqrt{\frac{2}{\pi}}\, \bar{G}\, S\, (2\pi wR')^{-1/2} \cos\left(2\pi wR' - \frac{\pi}{4}\right), \qquad (3)$$

where S is the flux contained in the ring. Although $S << S_o$ the visibility peaks generated by this component fall off much more slowly with wR' than in the case of a uniform disk. We do not expect a significant contribution from this effect since our antennas are of different size and do not have coincident nulls. This component may be worth consideration for other solar interferometric studies, however.

To test the possible effect of sidelobe variations in the observation of an extended source, we observed the Moon under the same conditions as the Sun. On April 29, when the Moon's apparent declination passed through 0^o, its center was tracked through the hour angle range -4 to 0 hr. No signal exceeding 10 Jy was observed at any time. Since the Sun is approximately 40 times brighter than the Moon at 8 mm, we estimate that if the solar brightness distribution were as uniform as that of the Moon we would have observed a signal less than 400 Jy. This confirms the reality of our observations and allows us to conclude that sidelobe variation effects cannot explain the solar results. However, since the Moon's limb darkening may differ significantly from that of the Sun,

there is some uncertainty in this limit.

b) Several Time Variable Sources or a Single Expanding Source

One alternative explanation for the observed fluctuations is that they are primarily due to several small time variable sources. A simple model which we first consider consists of a random pattern of 10-30 minute bursts from such sources which blink on and off like the lights of a Christmas tree. Several small intense sources may appear in the beam at any one time. As one source dies out another may brighten at a different point, producing a shift in the interferometer phase and a new peak in the amplitude.

First we note that there is a complete absence of large-scale events in all of the data taken within an hour of transit, while these events occur in most of the data taken at large hour angles. Conceivably the fluctuations occur in groups and the three periods during which transit data were obtained happened to coincide with quiet periods. We consider it unlikely, however, that this coincidence would happen on three successive days with the observed symmetry about transit. We may also suppose that the variable sources are resolved at the 30" fringe spacing obtained near transit, but not at the 40" or larger spacings where the events occur frequently. The sources must therefore be both tightly constrained and markedly uniform in size, and they must brighten and fade uniformly across their surfaces.

The frequently occurring nulls present another difficulty for this model. A null will appear if the termination of one

burst happens to coincide with the start of a second and no other source is in the beam at the time. Also, if two events overlap in time and are located on lines of opposite interferometric phase, then a null will occur at the instant their fluxes become equal. It is unlikely that such coincidences can occur as often as they are observed in Figure 1 unless there exists a high degree of correlation among the sources in either position or time. As we discuss in the next section, these nulls are much more readily explained as zero crossings of visibility functions as in the case of Venus shown in Figure 5. Moreover, these visibility effects produce 180 degree phase shifts which are correlated with amplitude nulls.

Bocchia and Poumeyrol (1975) have proposed an alternate model for the observed variations in which a small source physically expands to cut across the interferometer fringes, thereby producing short-term visibility variations. They consider a geometry in which a uniformly bright disk grows in diameter from perhaps one to several fringes in size, producing peaks and 180° phase shifts in the observed signal as the source is progressively resolved. The decreasing amplitude of the successive maxima of the visibility function is compensated for by the fact that the source grows in total flux as the square of its radius.

The total flux from such a source, however, must be much larger than the visibility peak and will begin to contribute significantly to the mean Solar brightness temperature. Consider the double peaks observed around 3h on March 15, of magnitude ~5000 Jy (cf. Figure 4). If these were due to succesive lobes of the visibility function of a growing disk, the disk itself must contribute a flux which increases by about 50,000 Jy from one peak to the next. We calculate that the corresponding

increase in antenna temperature in the larger of our two antennas would be $\Delta T_A > 200$ K. The total power received by the 5.5-meter antenna was monitored by chart recorder during the observations, and the record for the period including this event is shown in Figure 6. The occasional pulses are equivalent to a change $\Delta T_A = 56$ K and are obtained by the periodic injection of noise power from a gas discharge tube weakly coupled to the input of the radiometer. The total power received by this antenna is uncompensated, and is subject to gain drifts and variations in atmospheric attenuation which may amount to 50 K/hour. The small, high frequency variations are caused by second order effects due to the local oscillator frequency offset device and delay line tracking. Apart from these known effects there is no evidence for a change in antenna temperature by as much as 200 K. We have examined this record for all other similar events, and in no case find evidence for fluctuations in antenna temperature exceeding 50 K. While this is marginally consistent with fluctuations from unresolved variable sources, it is inconsistent with an expanding disk model for the observed variations. We conclude that fluctuations due to expanding resolved sources give an unlikely explanation for our observations, and that total power records obtained during similar variations observed by others will probably lead to the same conclusion.

IV. CONCLUSION - INTERPRETATION OF OBSERVED VARIATIONS IN TERMS OF SOURCE STRUCTURE

Because the unique observed variations in amplitude and phase cannot be reasonably explained by instrumental effects, several time varying sources, or a single explanding source, we are led to the conclusion that the only tenable explanation of these variations lies in the changing effective baseline (or

fringe spacing) caused by the Earth's rotation during the observing period. We know that the observed interference signal must come from individual sources whose angular extents are less than 30", and attribute the changes in amplitude and phase of the signal as the visibility variations of a few such sources which may be distributed randomly in the antenna beam. The lobe-like appearance of the amplitude variations and the frequently occurring nulls which are often correlated with 180 degree phase shifts are naturally explained in terms of visibility structure. Moreover, the disappearance of large-scale events near transit, where in our geometry the fringes become constant, provides an essential confirmation of this explanation.

To be more specific, the exponential terms in the integrand of Equation 1 describe a pattern of sinusoidal fringes of spacing $(u^2 + v^2)^{-1/2}$, whose lines of constant phase are oriented at an angle $\tan^{-1} v/u$ with respect to the direction of increasing right ascension. The projected baseline lengths u and v are shown in Figure 7 for the first and last days of observation. The variation is primarily in the u dimension since the Sun was observed near 0° declination with an east-west baseline. The fringe pattern contracts and expands with very little rotation during the course of a day's observation, remaining nearly constant around transit, and identical at times equally displaced before and after transit.

Plots of the data in Figure 4 as a function of total baseline projection $w = (u^2 + v^2)^{1/2}$ indicate that the large-scale, apparently periodic events seen at large hour angles and short effective baselines (w = 3000 to 4000 wavelengths) have periods of $\Delta w \approx \Delta u \approx 500$. These events may be interpreted as due to brightness structure on the Sun. From the Fourier relationship of Equation 1, spatial structure in an interval $\Delta\eta$ will produce variations of width Δu in the transform coordinate u as given by

$$\Delta\eta \, \Delta u \approx 1 \, .$$

For typical large events with $\Delta w \approx \Delta u \approx 500$, we obtain the estimate

$$\Delta\eta \approx 1/500 \approx 7' \, .$$

Because the beam pattern $G_1 G_2^*$ has a half power beamwidth of 8' and drops to 1/10 power in a diameter of 14' it includes sources of separation $\Delta\eta$. The gross features of our observations are therefore consistent with fine scale brightness structure on the Sun contained within the main beam of the interferometer. The large-scale amplitude fluctuations observed away from transit may be explained as visibility variations caused by a few intense sources whose individual sizes are comparable to the fringe spacing (30") and which are randomly distributed in the beam with average angular separations of 7'. If we consider the largest flux peak Sn as due to perfectly constructing interference produced by a small number n of such sources, the average flux per source would be Sn/n. Taking the

largest observed peak Sn = 10^4 Jy on March 19, the average flux per source would be $\leq$ 5000 Jy. For a source diameter of 30", the equivalent brightness temperature would be approximately 7500 K or less. The net contribution of the brightness temperature of the Sun as seen in a beamwidth of 8' diameter would be about 200 K.

If the observed variations are caused by changing effective baselines while observing a matrix of small-scale features, and if these features are usually present on the surface of the quiet Sun, we would expect other interferometric observations at comparable wavelengths and angular resolutions to exhibit the same variations in amplitude and phase. Moreover, the variations should only be present when the effective baselines are changing quickly, and their periods should go roughly as λ/B, where λ is the observing wavelength and B is the effective baseline. In addition, the intensity of the variations should be roughly proportioned to λ^{-2} if the small-scale features are thermal radiators. Observations by Bocchia and Poumeyrol (1976) with λ = 8.6 mm and λ/B = 27" give amplitude variations with essentially the same periods and intensities as those reported in this paper - suggesting that the proposed matrix of small-scale features is a common feature of the quiet Sun. Observations by Kundu and Velusamy (1974) at λ = 1.3 cm and λ/B = 10" give amplitude variations with periods which are about three times as fast as those reported in this paper and slightly smaller intensities. These observations are therefore compatible with the visibility variation interpretation, and with the idea that the sources are thermal radiators. This interpretation

has been further substantiated by Lang and Willson (1977) who observed the quiet Sun between March 30 and April 4, 1977 with λ = 11 cm and λ/B = 36.7" and 10.5". They found that the peak intensity of the observed amplitude variations increases systematically with increasing hour angle, and that the variations are undetectable at source transit where the effective baseline is changing very slowly. When present, the nulls in the amplitude variations were often associated with 180 degree phase shifts. The periods of the amplitude variations at λ/B = 36.7" were on the order of those reported in this paper whereas the intensity of the variations was about 24 times smaller. This would be expected from the visibility variations of small-scale thermal radiators. The observations of Lang and Willson (1977) at λ = 11 cm and λ/B = 10.5" exhibit amplitude and phase fluctuations which are roughly three times as fast as those observed at λ = 11 cm and λ/B = 36.7", in agreement with the visibility variation hypothesis.

Although interferometric observations of the quiet Sun at millimeter and centimeter wavelengths with angular resolutions of tens of seconds of arc can be interpreted in terms of visibility variations while observing a few intense, small-scale features, a similar explanation cannot account for the amplitude variations observed at 3.7 cm wavelength with higher angular resolutions of a few seconds of arc (Lang 1974b). In the first place, these amplitude variations have durations of five to ten minutes whereas they would have to vary on time scales of less than a minute if they were due to the visibility

variations mentioned in this paper. Moreover, the complex source structure required for variations of about five minutes with angular resolutions of a few seconds of arc would lie well outside the main beam of the interferometer used to record the variations. Secondly, both Lang and Willson (1977) and Kundu and Alissandrakis (1975) have used observations when the Sun is near vernal equinox to show that these amplitude variations are present during solar transit when the effective baseline changes very slowly. Because the intensity of the variations are comparable to the intensities of the tens-of-second-of-arc structures, it is unlikely that the smaller-scale variations are due to pointing or tracking errors while tracking these structures. It is more likely that the amplitude variations seen with interferometers operating at 3.7 cm wavelength with angular resolutions of a few seconds of arc are due to individual time-variable, fluctuating sources whose sizes are comparable to the interferometer's fringe spacing. In this view, interferometric observations of the quiet Sun at millimeter and centimeter wavelengths have revealed two types of ubiquitous small-scale features. One type has angular sizes of a few arc seconds and probably undergoes intrinsic fluctuations with time scales of minutes, whereas the other type has angular sizes of tens of seconds of arc and produces visibility variations with time scales of tens of minutes. It is the latter component which has been the primary topic of this paper.

REFERENCES

Bocchia, R. and Poumeyrol, F. 1974, Solar Phys. 38, 193.

Bocchia, R. and Poumeyrol, F. 1976, Ap. J. 204, L 107.

Delannoy, J., Lacroix, J., and Blum, E. J. 1973, Proc. Inst. Elec. Electron. Engrs. 61, 1282.

Hills, R. E., Janssen, M. A., Thornton, D. D., and Welch, W. J. 1973, Proc. Inst. Electron Engrs. 61, 1278.

Janssen, M. A., Gary, B. L., Gulkis, S., Olsen, E. T., Soltis, F. S., Yamane, N. I., 1977, in preparation.

Janssen, M. A. 1973, Science 179, 994.

Kundu, M. R. and Alissandrakis, C. E. 1975, M.N.R.A.S. 173, 65.

Kundu, M. R. and Velusamy, T. 1974, Solar Phys. 34, 125.

Lang, K. R. 1974a, Solar Phys. 36, 351.

Lang, K. R. 1974b, Ap. J. 192, 777.

Lang, K. R. and Willson, R. F. 1977, "Small-Scale Features of the Quiet Sun at 11 cm Wavelength" submitted to Ap. J.

FIGURE LEGENDS

Fig. 4. Signal phase and amplitude vs. hour angle for all solar data obtained. Universal time and date are indicated for each day. The lines are drawn from data obtained in 30 second integrations (10-sec integrations for the first record of March 15). The phase data possess a 360° ambiguity. Nulls or near-nulls in the signal are seen to frequently occur.

Fig. 5. Phase and amplitude obtained on Venus during the period of the solar observations. Venus was resolved by the interferometer during these observations, and its visibility function changes from positive to negative values. The data show a corresponding null in signal amplitude and a 180° shift in phase at the zero crossing. The instrumental noise quality and phase stability are indicated by these data. The observed amplitude fluctuations are consistent with system noise, and would be expected to increase by about only a factor of four when observing the Sun.

Fig. 6. Total power record of the 5.5-meter antenna taken during a double-peaked event on March 15. The times of the two amplitude maxima and the interventing null are indicated. The occasional pulses in the record are due to an artificial noise source calibrated to give an antenna temperature of 56 K. The high-frequency noise and occasional steps in the signal have known instrumental causes. Long-term instrumental gain variations are expected to be less

than 50 K during this period. There is no evidence for a power fluctuation > 50 K due to a variable source on the Sun.

Fig. 7. Variation of the baseline projections u and v with hour angle. Hour angle is indicated by tick marks and numbers on the curves. The u-v diagrams are shown for the first and last days of observation. On the day of vernal equinox (March 21) the baseline projection is nearly constant in the two hour period around transit. During this time the relative phase change between points separated by 8' on the plane of the sky would be less than 1^{o}.

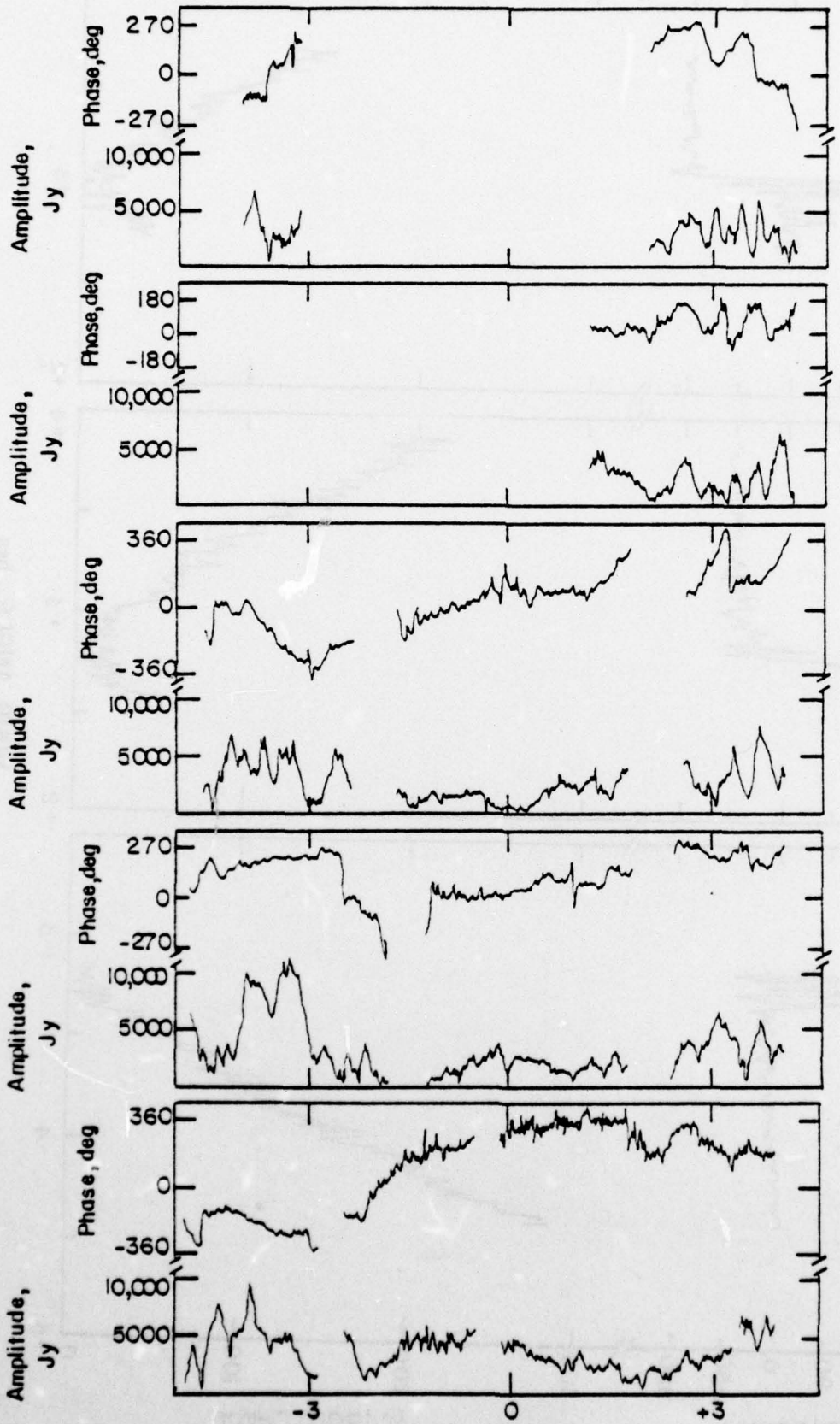

Phase, deg
270
0
-270
Amplitude, Jy
10,000
5000
Phase, deg
180
0
-180
Amplitude, Jy
10,000
5000
Phase, deg
360
0
-360
Amplitude, Jy
10,000
5000
Phase, deg
270
0
-270
Amplitude, Jy
10,000
5000
Phase, deg
360
0
-360
Amplitude, Jy
10,000
5000
-3
0
+3
HOUR ANGLE, hrs

FIGURE 4.

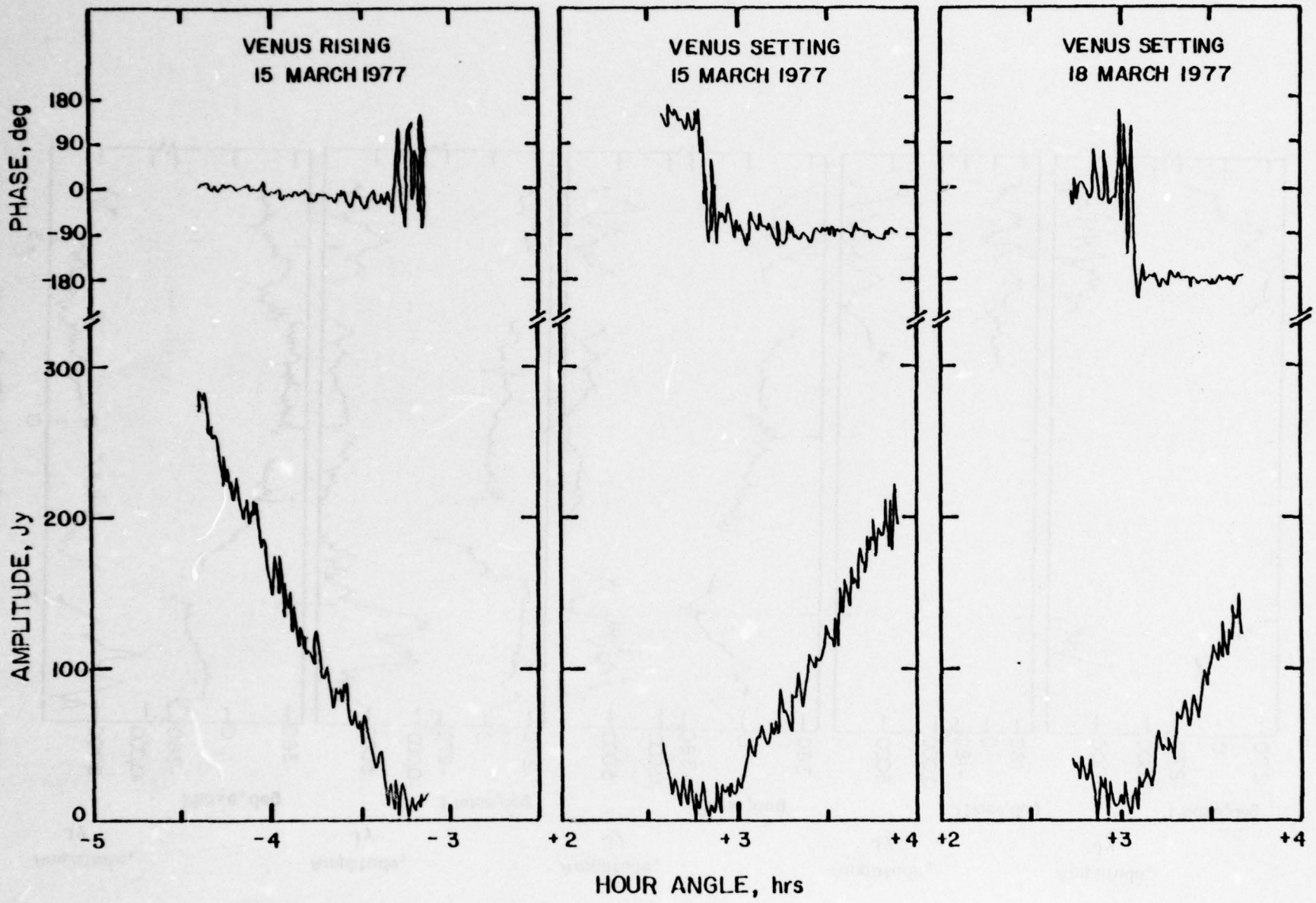

VENUS RISING
15 MARCH 1977
VENUS SETTING
15 MARCH 1977
VENUS SETTING
18 MARCH 1977
PHASE, deg
180
90
0
-90
-180
AMPLITUDE, Jy
300
200
100
0
-5
-4
-3
+2
+3
+4
+2
+3
+4
HOUR ANGLE, hrs

Figure 5.

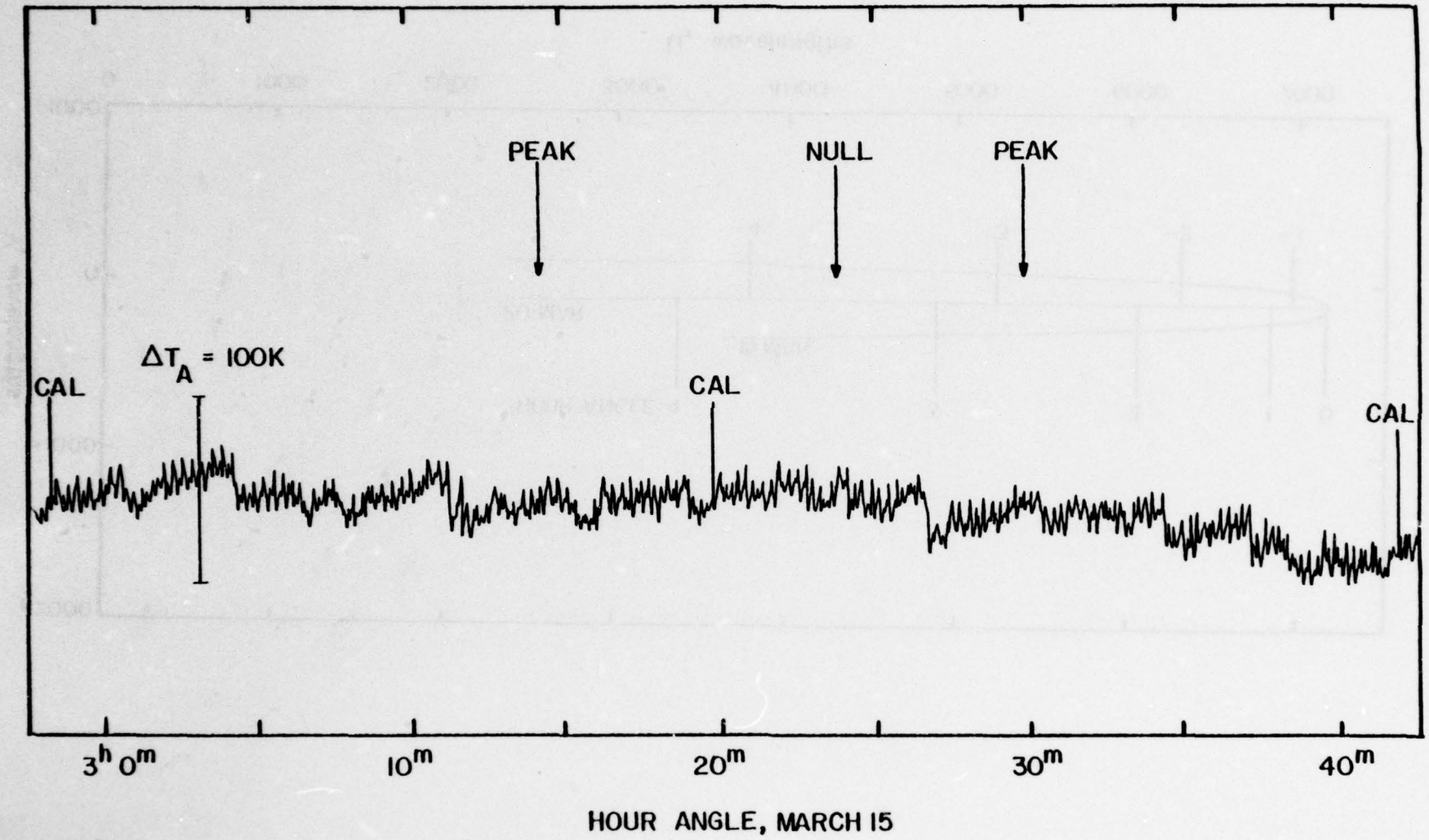

PEAK
NULL
PEAK
CAL
ΔT_A = 100K
CAL
CAL
$3^h\,0^m$
10^m
20^m
30^m
40^m
HOUR ANGLE, MARCH 15

Figure 6.

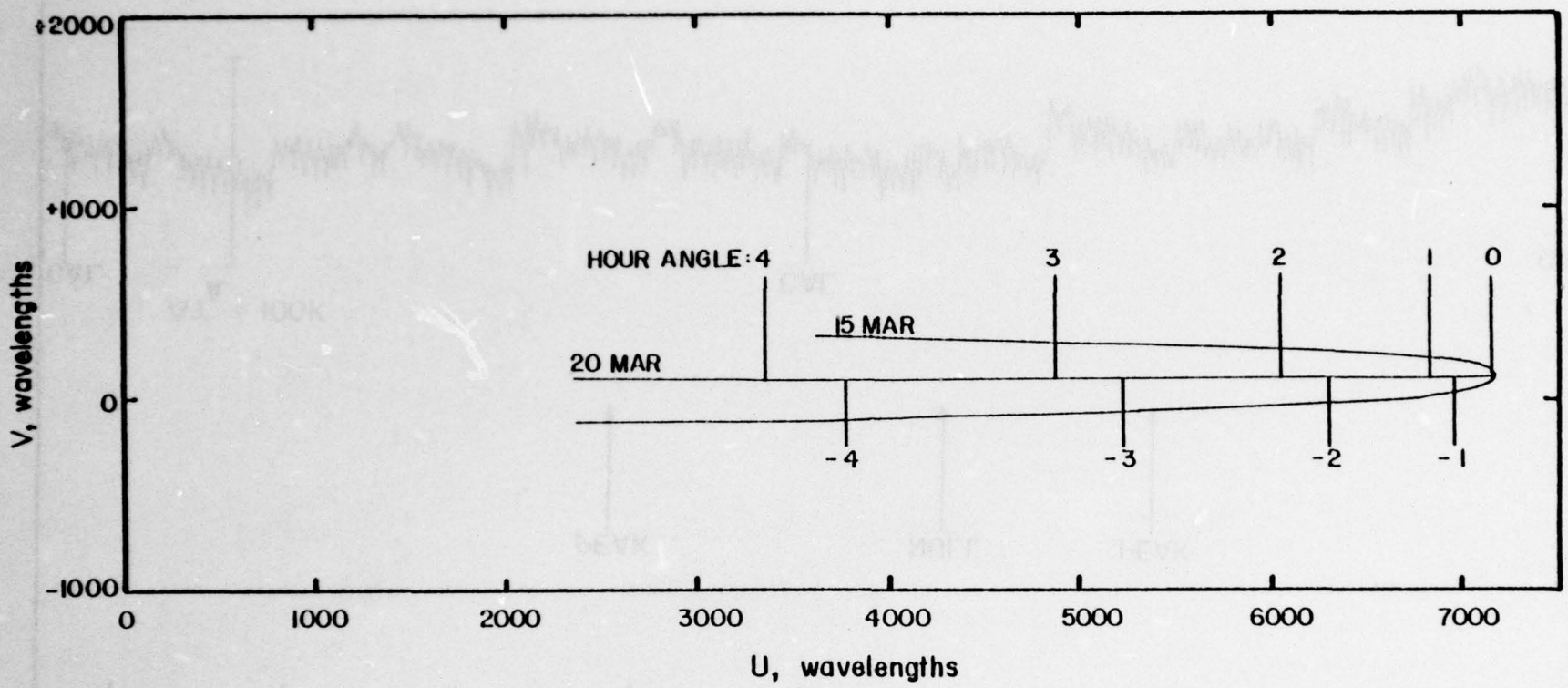

+2000
+1000
0
-1000
V, wavelengths
HOUR ANGLE: 4
3
2
1
0
15 MAR
20 MAR
-4
-3
-2
-1
0
1000
2000
3000
4000
5000
6000
7000
U, wavelengths

Figure 7.

E. HIGH RESOLUTION INTERFEROMETRIC OBSERVATIONS OF SUNSPOTS AT 3.7 AND 11 cm WAVELENGTH

When sunspots (or active regions) are present on the solar surface they dominate the solar emission at centimeter wavelengths. Although the angular sizes of sunspots are comparable to the beamwidths of large single radio telescopes (a few arc minutes), Lang (1974) has shown that most of the sunspot emission at centimeter wavelengths comes from sources which are only seconds of arc in size. Interferometric observations of sunspots at centimeter wavelengths have shown that these intense, small-scale features are remarkably stable with angular sizes, intensities and degrees of circular polarization which remain essentially constant for days. This stability makes these features ideal objects for synthesis maps in which data taken during one day can be used to delineate the core-halo and circular polarization structures of sunspots. These structures can in turn be used to study the magnetic field structure in the coronal regions where the centimeter wavelength emission originates. Of special interest are day to day and hourly changes in the brightness and circular polarization structures. Observations taken in November of 1975 showed that the circular polarization of a sunspot changed dramatically by 100 percent prior to the emission of a flare. We believe these changes are caused by emerging magnetic fields which trigger solar flares (Lang, 1977).

We have observed the sunspot region 757 with the three element interferometer of the National Radio Astronomy Observatory between November 18 and 22, 1976. During this period the sunspot travelled from the limb of the Sun to its center and during this period no flare activity was reported by any optical or radio observatory. Observations were taken with a dual channel system at signal frequencies of 2695 MHz (λ = 11 cm) and 8085 MHz (λ = 3.7 cm) with circularly polarized feeds and an intermediate frequency bandwidth of 30 MHz. The 10^4 K signal from the Sun dominated the system noise and gave an r.m.s. noise error

in fringe amplitude of 10 Jy (1 Jy $=10^{-23}$ erg s^{-1} cm^{-2} Hz^{-1}) for our integration time of 30 seconds. Both fringe amplitude and phase were sampled every 30 seconds at alternate signal frequencies, and this data has been used to construct maps of the sunspot regions. In subsection a) which follows we describe the basic techniques used in constructing these maps, whereas in subsection b) we present and briefly discuss maps taken at 11 cm wavelength on two different days each with two different polarizations. We are now in the process of making similar 3.7 cm maps, and the November 1975 data is being resurrected from archival tape for the production of similar maps. In this case a flare did occur and comparisons of maps taken at different times with different polarizations should lead to interesting conclusions regarding the physics of the solar flare process. All of these maps will be collected together in a paper with this section's title which will be submitted to Solar Physics in September.

a) Mapping Techniques

The fundamental relationship between the brightness distribution I(x,y) and interferometric observables is

$$(1) \qquad V(u,v) = \int I(x,y)\, e^{-2\pi i(ux+vy)}\, dxdy .$$

Here V(u,v) is the so-called visibility function whose amplitude and phase are the observed fringe amplitude and phase; u and v are the projection of the baseline vector in the direction of increasing right ascension and declination, respectively; x and y are, respectively, coordinates in the direction parallel to increasing right ascension and declination. These quantities, defined in radians, are given by

$$(2) \qquad u = \frac{B}{\lambda}\ (\cos\delta_b \sin(\mathrm{LHA} - \mathrm{BHA}))$$

$$v = \frac{B}{\lambda}\ (\sin\delta_b \cos\delta_s - \cos\delta_b \sin\delta_s \cos(\mathrm{LHA} - \mathrm{BHA})),$$

where δ_b and δ_s are the declination of the baseline vector and of the source, respectively, LHA and BHA are the local hour angle of the source and the baseline, and B and λ are the magnitude of the baseline vector, and the wavelength of observation. The baseline declination and hour angle depend on the geocentric components, B_x, B_y, and B_z of the baseline vector, viz:

$$\delta_b = \text{Arctan}\left(\frac{B_z}{(B_x^2+B_y^2)^{\frac{1}{2}}}\right)$$

$$\text{BHA} = \text{Arctan}\left(\frac{B_y}{B_x}\right) .$$

For the Green Bank interferometer, $\delta_b \sim 22^\circ$, and BHA$\sim$4.8 hours, for all three baselines.

As the earth rotates, and the local hour angle of the source changes, the projected baseline describes an ellipse in the uv plane. The ellipse is centered at $u = 0$, $v = \frac{B}{\lambda} \sin\delta_b \cos\delta_s$, has eccentricity $\cos\delta_s$ and semi-major axis equal to equatorial component of the baseline. Figure 8 shows the u-v tracks for each of the baselines at 11 cm. On November 18 the Sun's declination is -22°, and the tracks are fairly wide open. Near the equinox, $\delta_s \sim 0$, and the curves would degenerate into straight lines parallel to the v axis. The minimum fringe spacing at 11 cm is $\sim$ 8.5". If the u-v plane were sufficiently sampled then one could take the inverse transform of equation 1 to obtain the brightness distribution. If the source had a maximum angular extent Δx and Δy in right ascension and declination, then one need only make observations at intervals of $u \sim \frac{1}{\Delta x}$ and $v \sim \frac{1}{\Delta y}$, to obtain a unique map of the source. Since the source brightness is a real function, it follows from Equation 1, that $V(u,v) = V^*(-u,-v)$, so we need only measure V(u,v) on one half of the

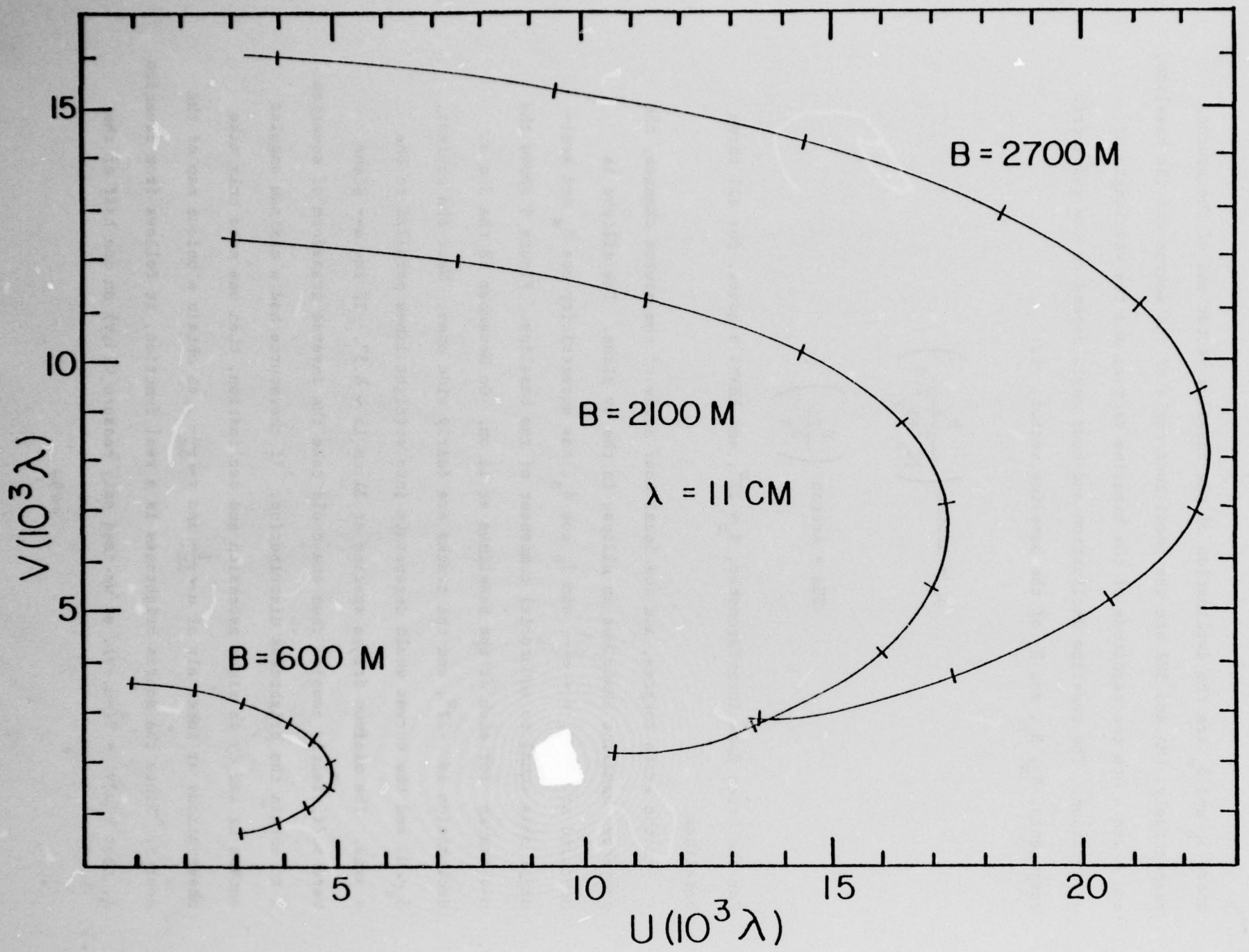


Figure 8. THE U-V TRACKS AT 11cm ON NOV. 22, 1976.

u-v plane. In practice, however, there are never enough interferometer pairs to satisfy the sampling criterion, and so one must resort to using some other technique for obtaining a map.

The procedure which we have implemented was first developed by Hogbom (1974) and is used widely in the mapping of extragalactic radio sources and also by Kundu and Alissandrakis (1977) to map solar active regions. In this scheme one calculates a direct synthesis "dirty map"

$$D(x,y) = \frac{1}{N} \Sigma A_i \cos \phi_i + 2\pi(ux+vy) , \tag{3}$$

where A_i and ϕ_i are the amplitude and phase of observation i, N is the number of observations, and x and y are positions located on a grid of coordinates of the sky. Since the visibility function is symmetric, only the real (cosine) part of the transform need be calculated. The dirty map is the convolution of the true brightness distribution with the response function of a point source. This response function or "dirty beam" is the Fourier transform of the sampling function and is given by

$$B(x,y) = \frac{1}{N} \Sigma \cos (u_i x + v_i y) w_i , \tag{4}$$

where w_i is the weight given to each data point.

Figure 9 shows the dirty beam pattern at 11 centimeters constructed using one days worth of November 1976 observations with uniform weighting $w_i = 1$. The half power width is 4" x 20" and the highest sidelobe is 20% of the maximum response. One could alter the beam pattern by adjusting the weights. If the outer spacings were more heavily weighted, the beamwidth would become smaller, but at the expense of higher sidelobes. Weighting the inner spacings more heavily would broaden the main beam but decrease the inner sidelobes.

The deconvolution can be performed by means of the "clean" procedure described by Hogbom (1974) in which the brightness distribution is decomposed into a sum of beam patterns. The dirty map is searched for the maximum and a

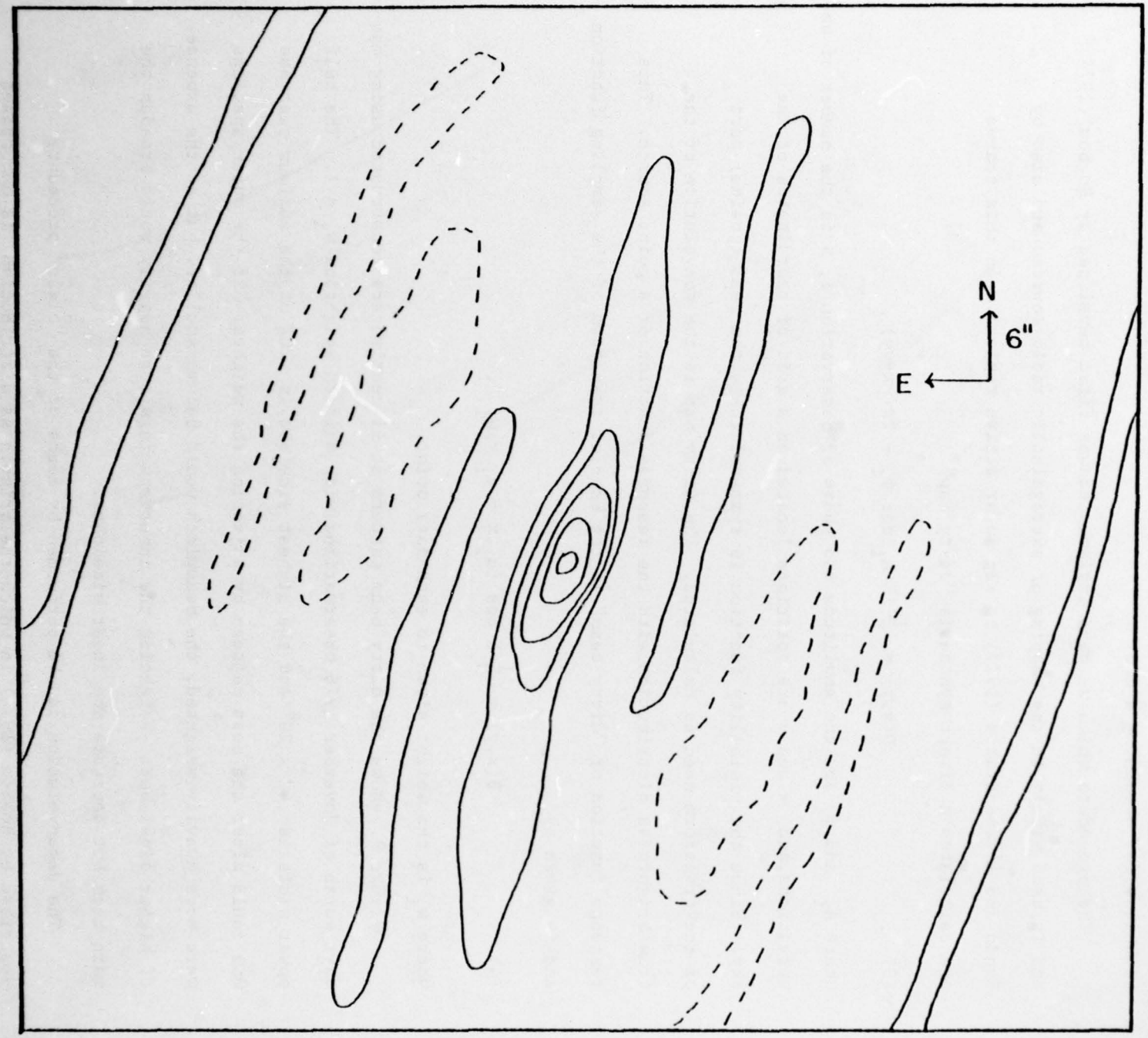


Figure 9. , BEAM PATTERN AT 11cm ON NOV. 22, 1976.

point source is fit to the map at that point

$$\text{Amp} = \frac{\sum_{j=1}^{n} \sum_{i=1}^{m} \frac{D_{ij}}{B_{ij}} (B_{ij})^2}{\sum_{j=1}^{n} \sum_{i=1}^{m} B_{ij}^2} .$$

Here i and j correspond to positions on the grid. In our computer program, the grid is a 40 x 40 array with a specified spacing in Δx and Δy.

The dirty map usually has a number of disturbing sidelobes caused by insufficient sampling, but if we find that it is identical in every detail to the dirty beam then we know that the brightness distribution consists of a point source at the position of the maximum on the map. If this dirty beam pattern is then subtracted from the dirty map then there should be nothing left. If a "clean" beam pattern, i. e., the ideal main beam of a similar shape but without the sidelobes, is returned to the position, then the result will be the same as that which would have been obtained with normal synthesis if the relevant region in the u-v plane had been observed. Normally the point source response multiplied by some small fraction of Amp, (usually between .2 and .5) centered on the maximum in the map is subtracted from the dirty map. This procedure is repeated a large number of times until all of the significant noise is removed from the map.

b) Maps of a Sunspot Region at 11 cm Wavelength

In Figures 10, 11, 12 and 13 we present high resolution maps of a sunspot region taken at 11 cm wavelength with right and left hand circular polarizations on November 20 and 22, 1976. The structure is extended in the east-west direction where the beam pattern provides maximum resolution. North is in the upward direction, east is to the left, and the length of the arrows denoting direction correspond to 3 seconds of arc. The contours are surface brightness in units of Jansky per square arc second with a maximum value of about eight. The total

correlated flux was about 1,000 Jy on November 20 and about 400 Jy on November 22.

These maps show that the centimeter wavelength emission from sunspot regions is dominated by a few intense, small scale features with angular sizes of a few seconds of arc and circular polarizations on the order of sixty percent. The sense of the polarization is, however, different for different small-scale features. For example, in Figures 10 and 11 component I is about 60% right circularly polarized, component II about 25% right circularly polarized, and components III and IV are both about 60% left circularly polarized. Similar polarizations were seen two days previously for components I, II and III (Figures 12 and 13), but component IV was essentially unpolarized then. For a given day the total flux seen at the two polarizations is the same with different brightnesses for different components at different polarizations.

Our general conclusions regarding the dominant small-scale, circularly polarized emission regions in sunspots are similar to those of Kundu et al. (1977) who mapped different sunspot regions at 6 cm wavelength with 6 arc-second resolution using the Westerbork Synthesis Radio Telescope. They also found second of arc features with circular polarizations up to 60 percent, and they also observed an inversion of the sense of circular polarization in part of a bipolar magnetic field structure. Our results are, however, in the preliminary stage, for we want to obtain 11 cm maps for the other days of observation and 3.7 cm maps for all of the observation days. Comparisons of the 3.7 and 11 cm maps should lead to descriptions of polarizations at different heights. We also hope to obtain the exact positions of each of the small-scale components and to compare these features with optical photographs and magnetograms of the same sunspot region. Moreover, all of these things will be done for the November 1975 sunspot data which is now being obtained from N.R.A.O. archival tapes. Comparisons with gyroresonant absorption theory will also be made.

REFERENCES

Hogbom, J.A. 1974, Astron. and Ap. Supp. 15, 417.

Kundu, M.R., Alissandrakis, C.E., Bregman, J.D. and Hin, A.C. 1977, Ap. J. 213, 278.

Lang, K.R. 1974, Solar Phys. 36, 351.

Lang, K.R. 1977, Solar Phys. 52, 63.

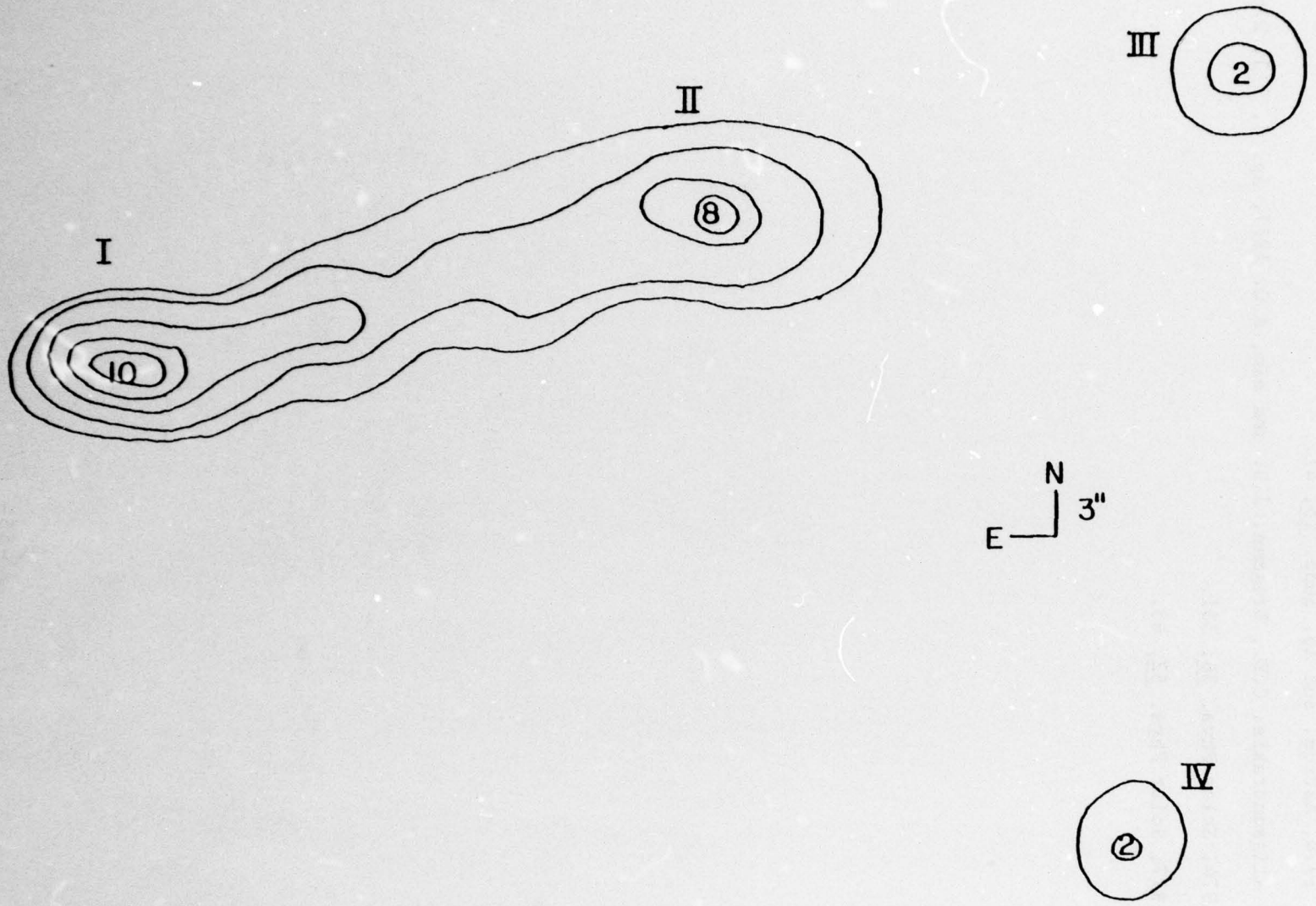


Figure 10. NOV. 22 - RIGHT CIRCULAR POLARIZATION

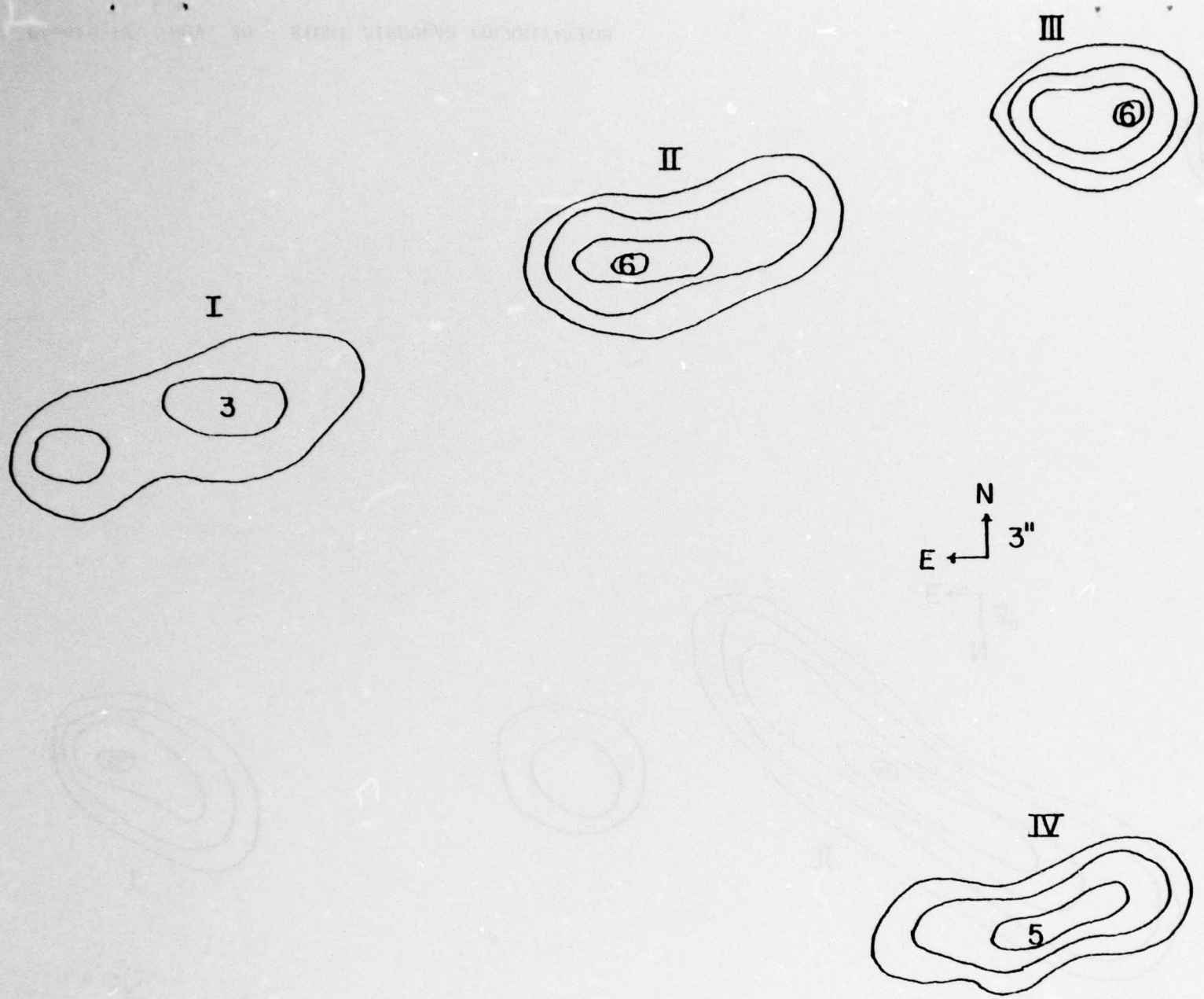


Figure 11. - NOV. 22 - LEFT CIRCULAR POLARIZATION

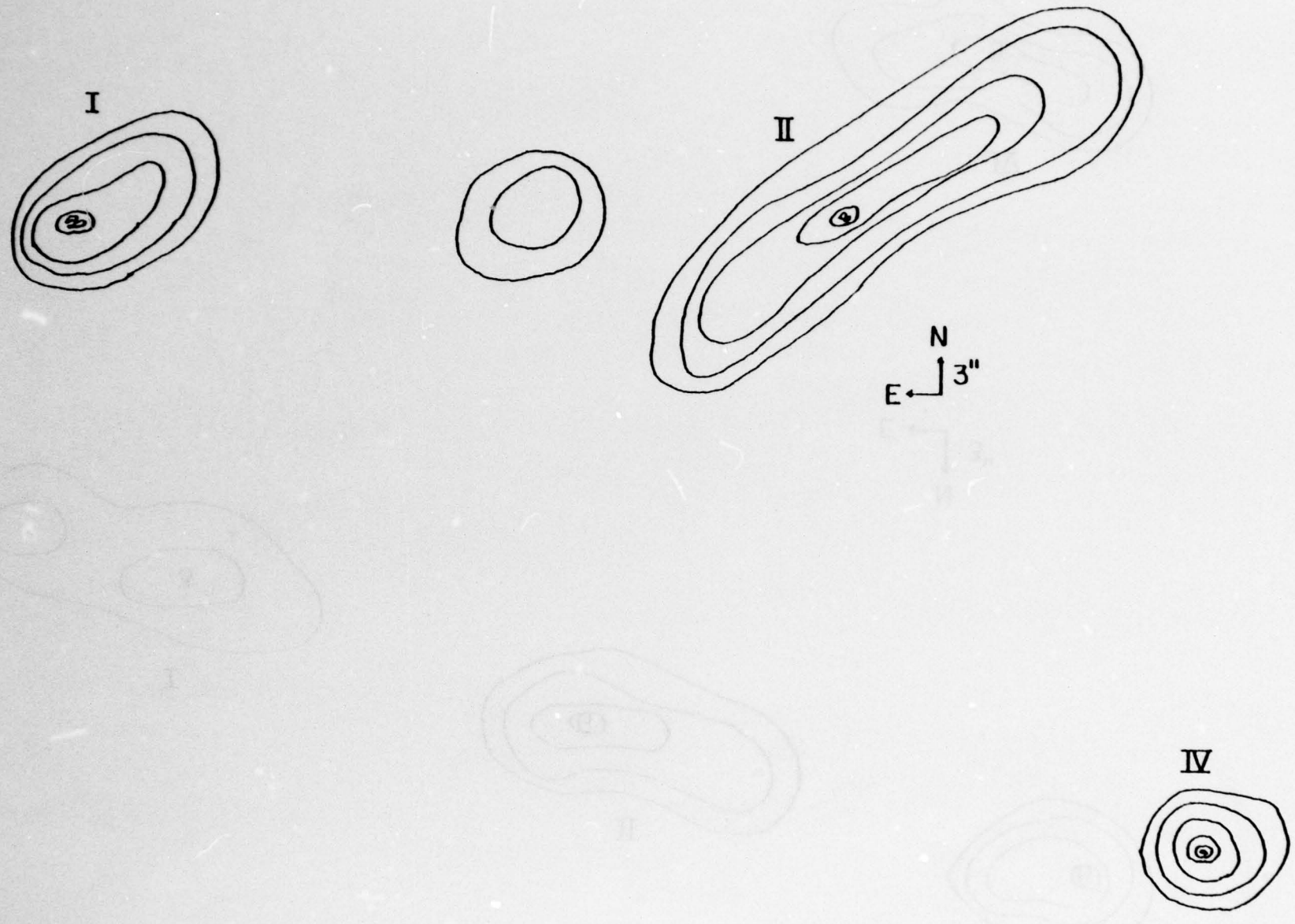


Figure 12. NOV. 20 - RIGHT CIRCULAR POLARIZATION

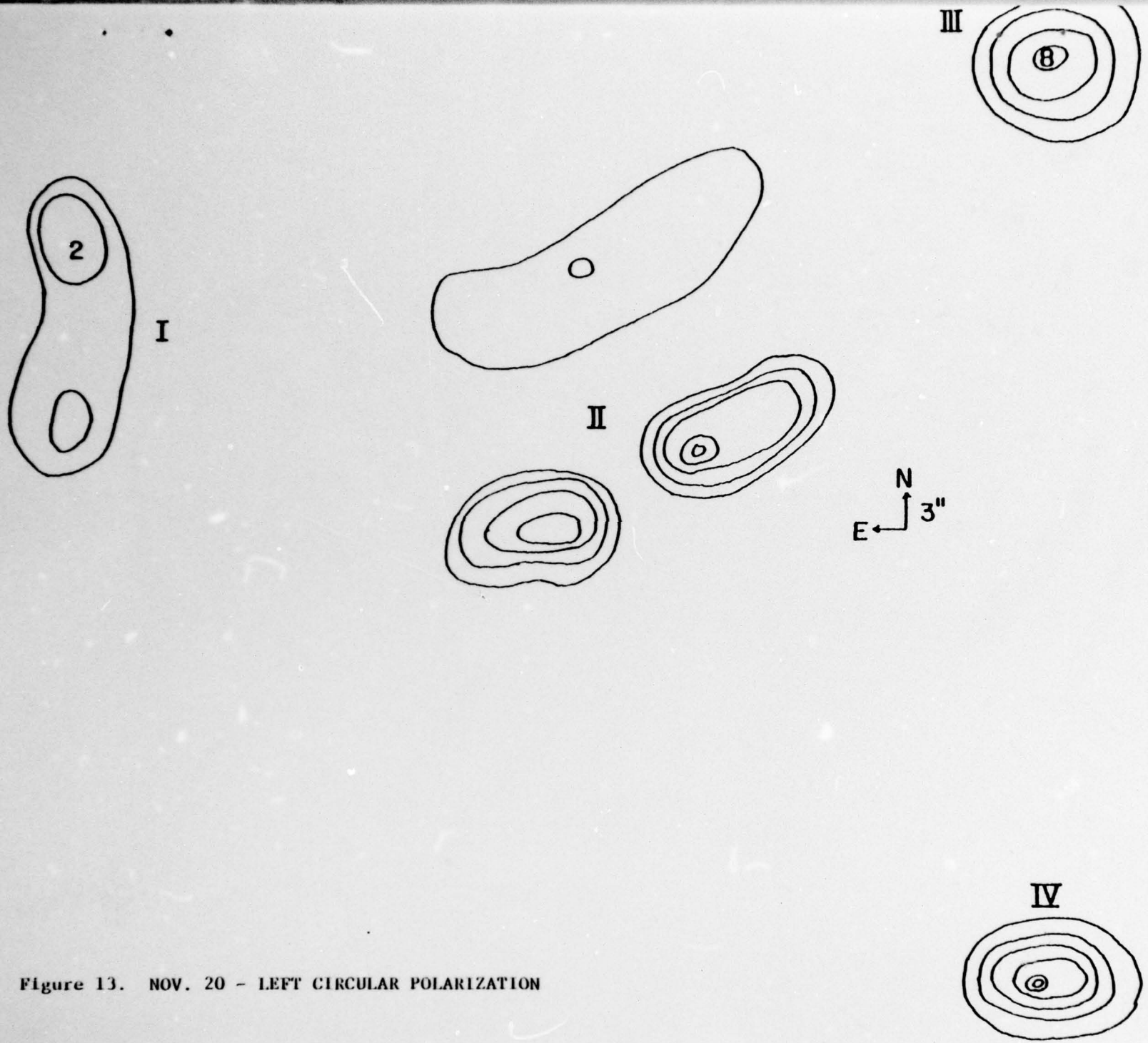


Figure 13. NOV. 20 - LEFT CIRCULAR POLARIZATION